



Numerical modeling of additive manufacturing: some thermomechanical aspects

Michel BELLET

Gildas GUILLEMOT, Charles-André GANDIN, Yancheng ZHANG

STEEL
SIM 2021

October, virtual conference

Introduction: L-PBF (laser beam melting)



Benefits...

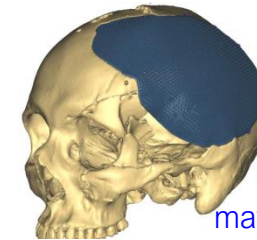
- Direct manufacturing of complex parts, based on CAD description
- Reduced time to market
- Light post-forming processes
- Wide application range in terms of materials



sirris.be

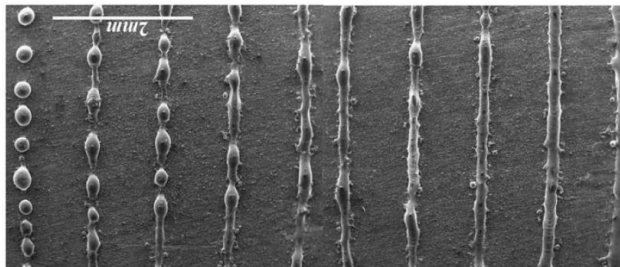


autodesk.fr

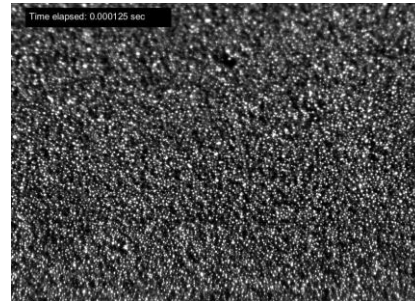


materialise.com

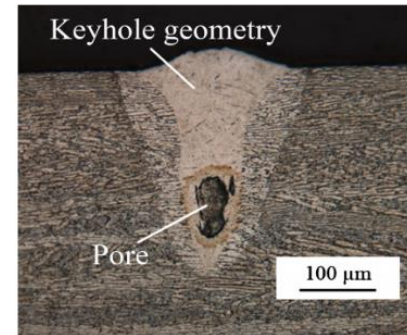
► ... but defects, at various scales, as results of complex multiphysics



"Balling", 316L, [Li et al. 12](#)



Vaporization and denudation, [Bidare et al. 18](#)



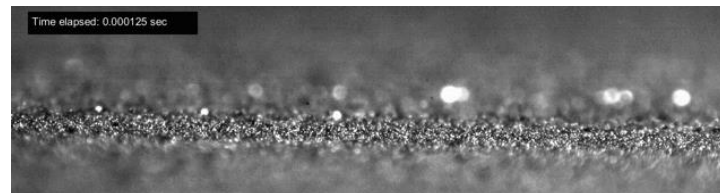
Porosities, [Gong et al. 14](#)



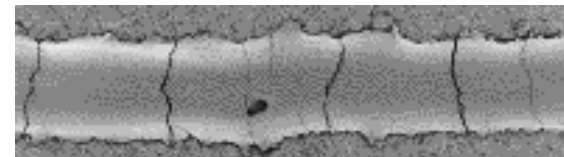
Cracks, [Merzelis & Kruth 06](#)



Lack of fusion, Ti-6-4, [Bandyopadhyay & Traxel 18](#)

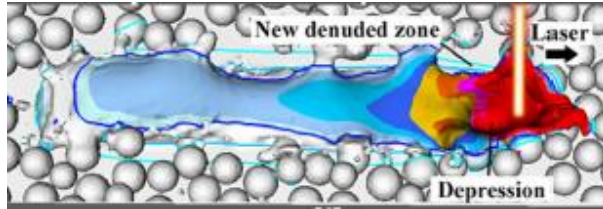


Microcracks Al₂O₃, [Moniz et al. 19](#)

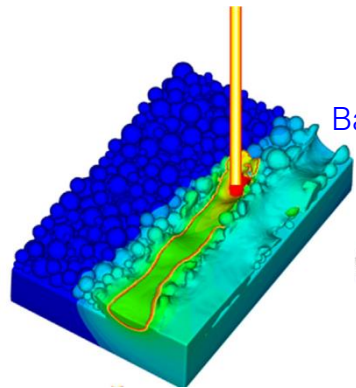


Numerical modeling: which scale?

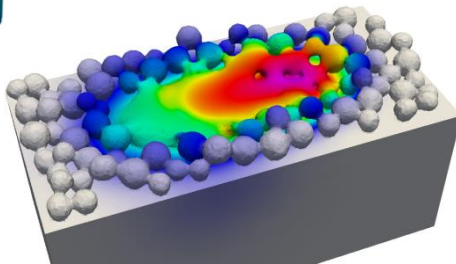
Particles scale – "microscopic"



Khairallah *et al.* 16



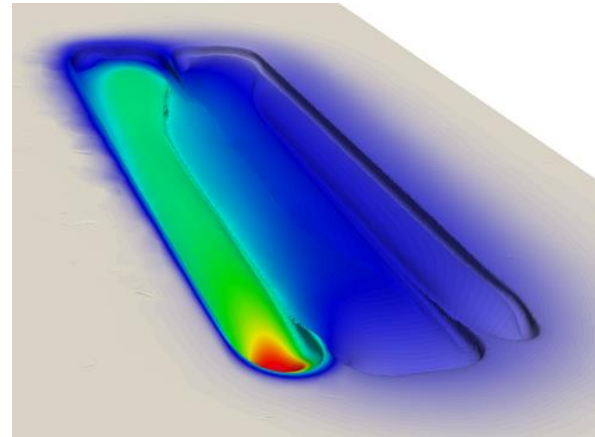
Bayat & Hattel 19



Zhang *et al.* 19, CEMEF

- Interaction laser – powder particles
- Formation of melted zone, porosities
- Influence of powder granulometry distribution
- Very high computing time

Track scale – Continuous powder bed "mesoscopic"

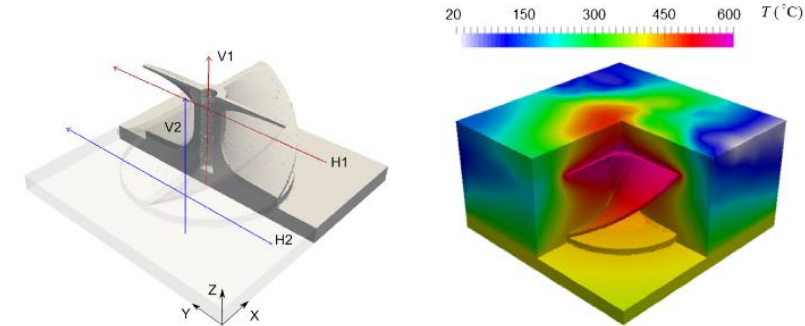


- Interaction laser – powder bed
- Balling, keyhole
- Shape of elementary deposits (tracks)
- Stress formation in the wake of the melted zone
- Hot cracking

Objective

Simulate L-PBF at meso- and macro-scale by FEM

Part scale "macroscopic"



Zhang *et al.* 19, CEMEF

- Temperature distribution
- Distortions and stress, during and after processing
- Cold cracking (solid state)

- ▶ L-PBF: Numerical simulation at the scale of elementary tracks
 - ▶ Thermohydraulics
 - ▶ Comparison with experimental testing, and validation
 - ▶ Thermomechanics
 - ▶ Focus on cracking risks: "cold" cracking, and solidification cracking
 - ▶ How to combine thermohydraulics and solid mechanics?
 - ▶ How to identify material behavior in processing conditions?
- ▶ Conclusions & perspectives



Meso approach: thermohydraulics

Meso approach for L-PBF

► Level set framework for unsteady thermohydraulics

■ Domains

- Multiphased domain : the material Ω_M
- Monophased domain : gas Ω_G

■ Interface between domains Ω_M and Ω_G

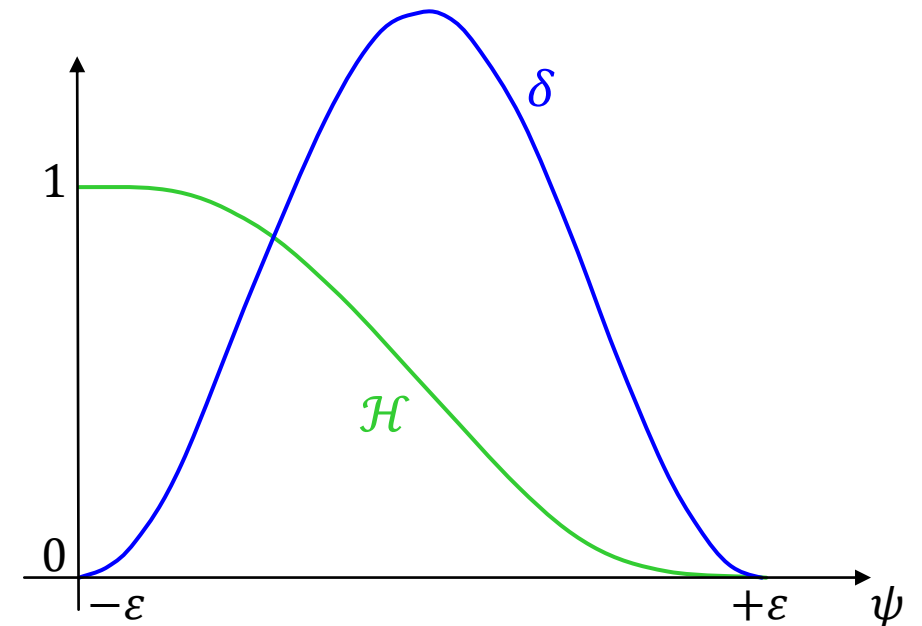
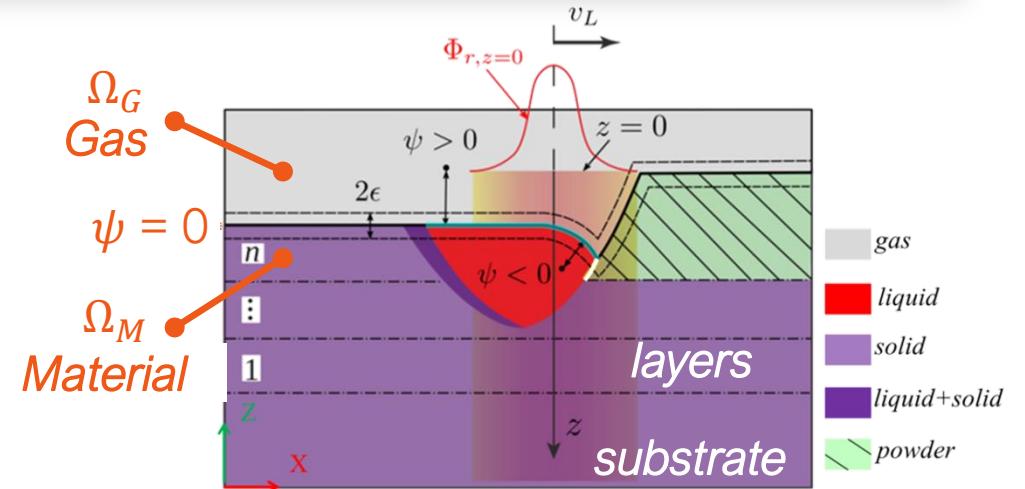
- Signed distance function ψ . Interface: $\psi = 0$
- Smooth Heaviside function \mathcal{H} in the transition zone $\pm \epsilon$

■ Mixed quantities

- In the transition zone : $\{\chi\} = \mathcal{H}\langle\chi\rangle^M + (1 - \mathcal{H})\chi^G$

- In the material : $\langle\chi\rangle^M = \sum_{\text{phases } j} g_M^j \chi^j$

■ Smoothed Dirac function $\delta = \frac{\partial \mathcal{H}}{\partial \psi}$



Thermo-hydraulics: main features

Thermal Solver

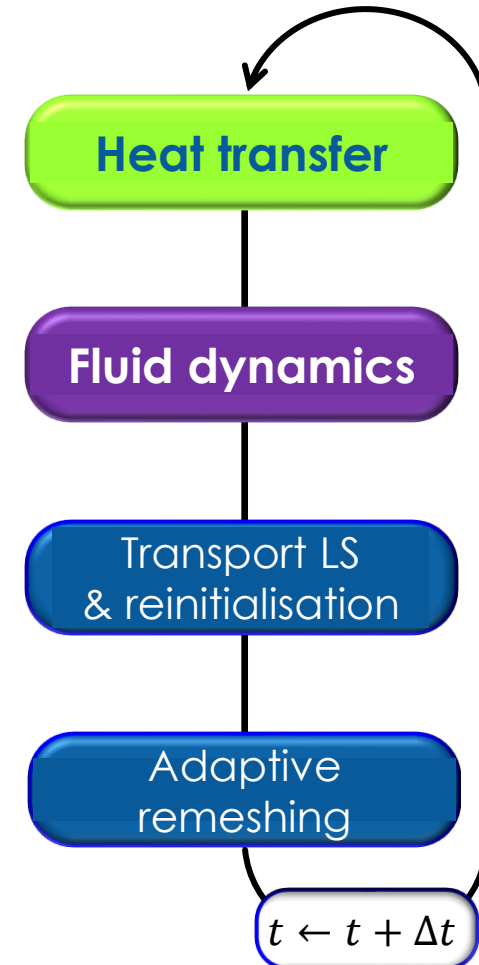
- Laser interaction
 - Heat input in surface on opaque liquids: Gaussian or “top-hat” distribution (+ CSF method, $\times \delta$)
 - Heat input in volume on semi-transparent liquids, or on powder bed: Beer-Lambert model

$$\frac{d\phi}{dz} = -\alpha\phi \quad \dot{Q}(z) = -\frac{d\phi}{dz} = \phi_{r,z=0}\alpha \exp\left(-\int_0^z \alpha dz\right)$$

- Heat loss, due to possible vaporization
- Models for apparent conductivity of powder beds

Navier-Stokes Solver (compressible)

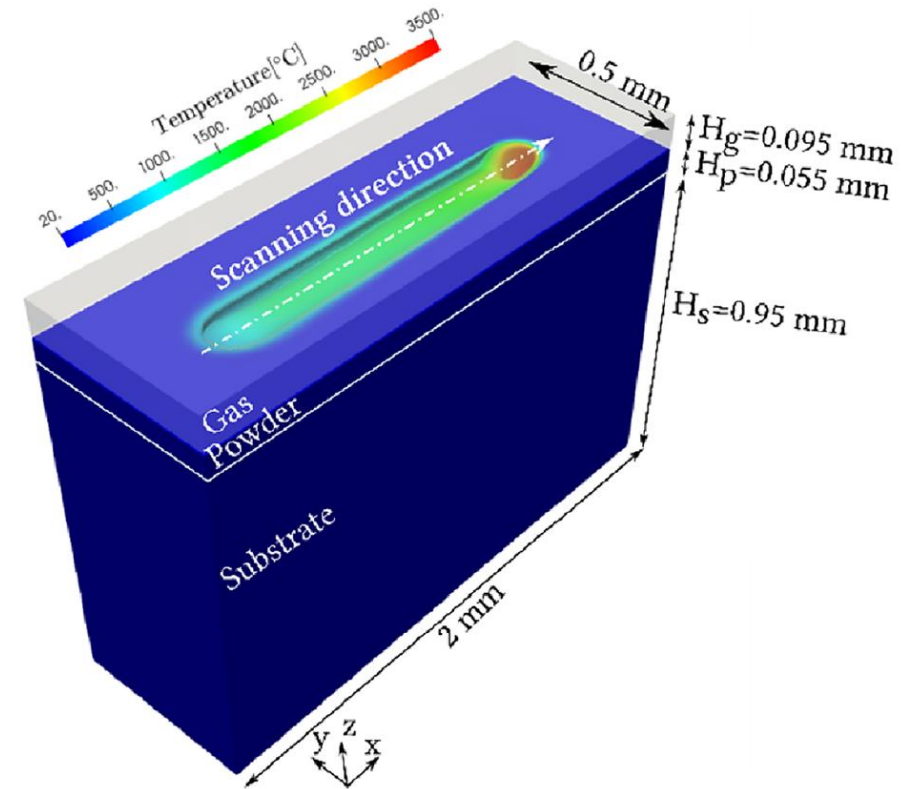
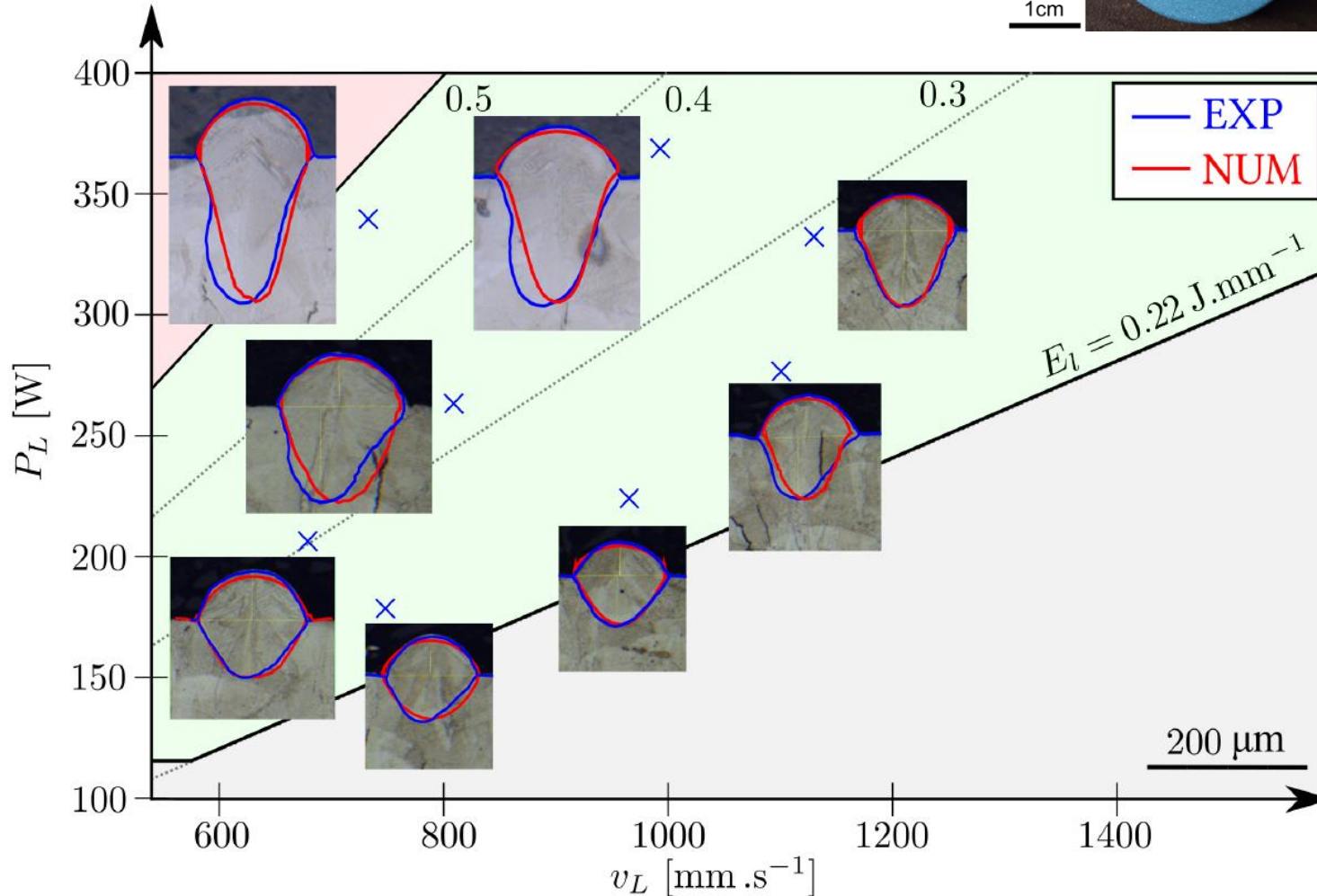
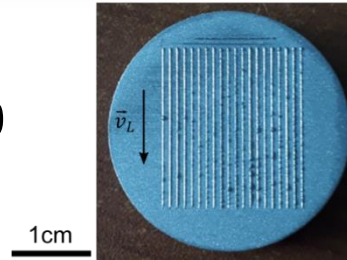
- Newtonian behavior
 - Transition powder / melted liquid: variation of $\langle \rho \rangle^M$ on a predefined interval ΔT
 - Laminar flow ($Re < 1000$)
- Applied forces
 - Gravity: $\{\rho\} \mathbf{g}$
 - Surface tension, including Marangoni: $\mathbf{f}_{ST} = \gamma \kappa_t \mathbf{n}_l + \frac{\partial \gamma}{\partial T} \nabla_s T$ ($\times \delta$)
 - Recoil pressure, due to possible vaporization



Simulation vs experiments for metals: IN738



Experiments: PhD of David Grange, 2020
Centre des Matériaux – Mines Paristech



Numerical simulation: PhD of Alexis Queva, 2021, CEMEF



Dynamic mesh adaptation

Multi-objective mesh adaptation

Coupez, J. Comp. Physics 2011

based on:

- Density (A)
- & Liquid fraction (B)
- & laser interaction zone

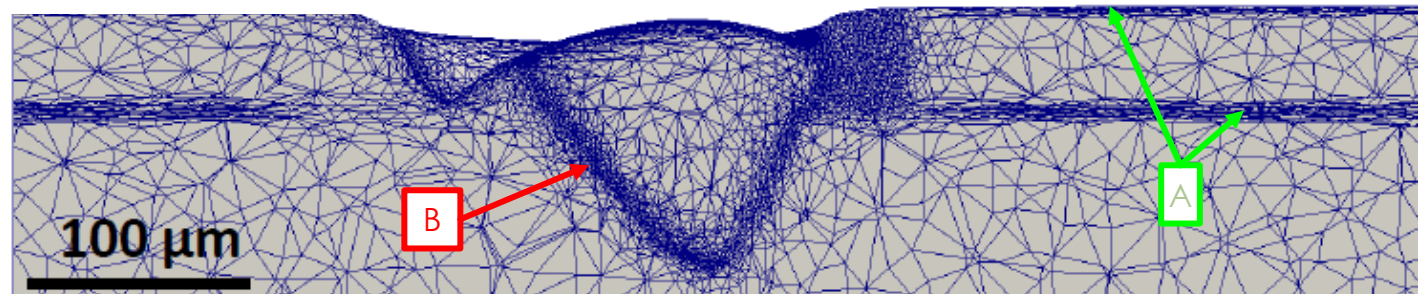
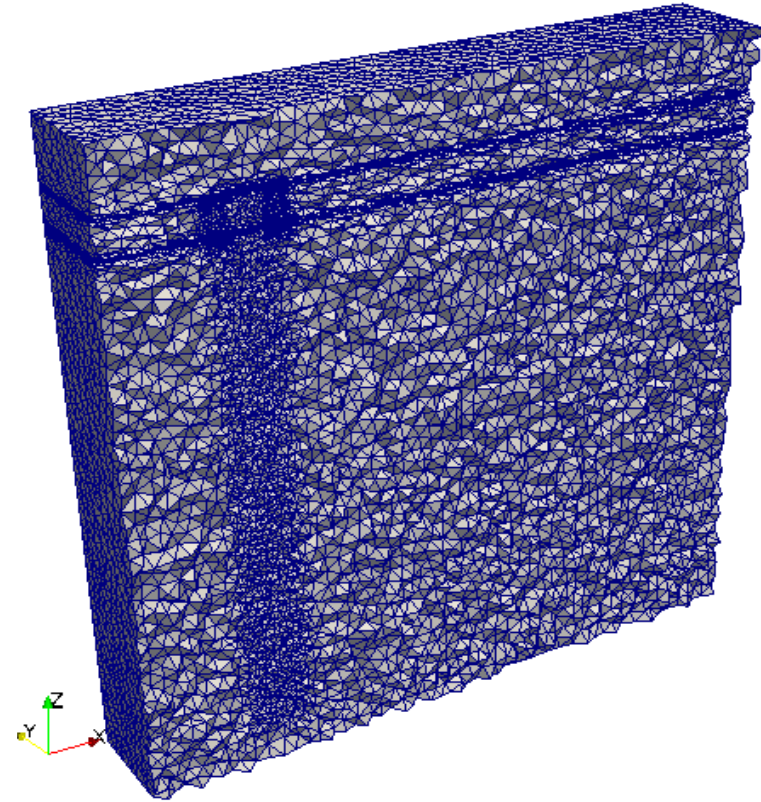
Background size: 50 μm

Min size : 0.5 μm

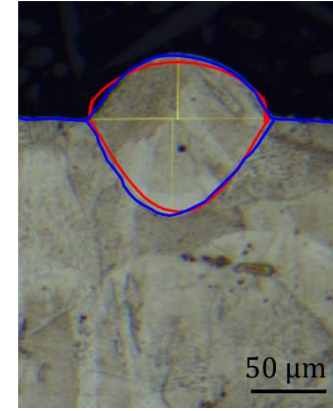
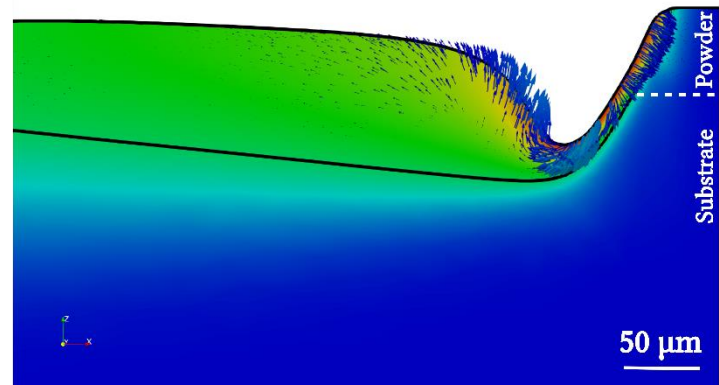
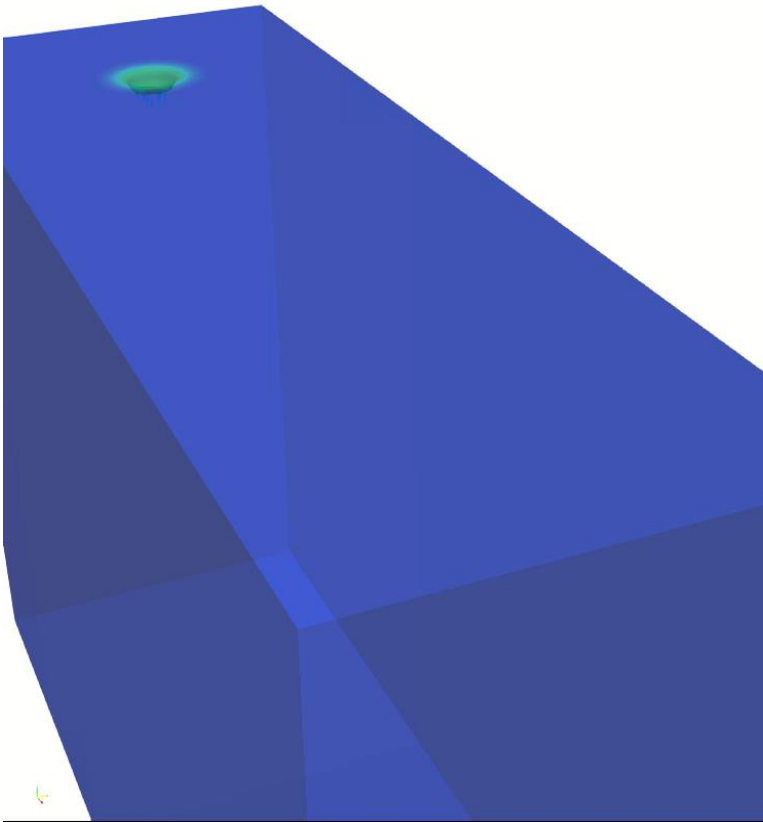
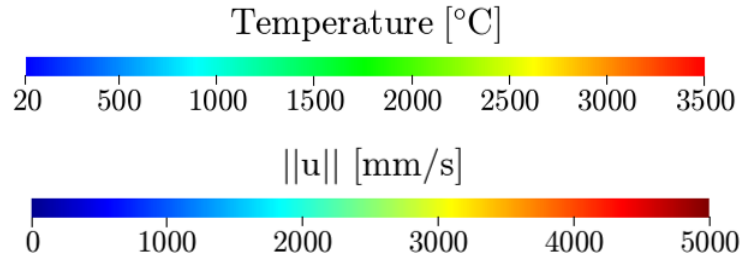
Remeshing period 10 μs

$$N_{Eelts}(t_0) = 2.1 \text{ M}$$

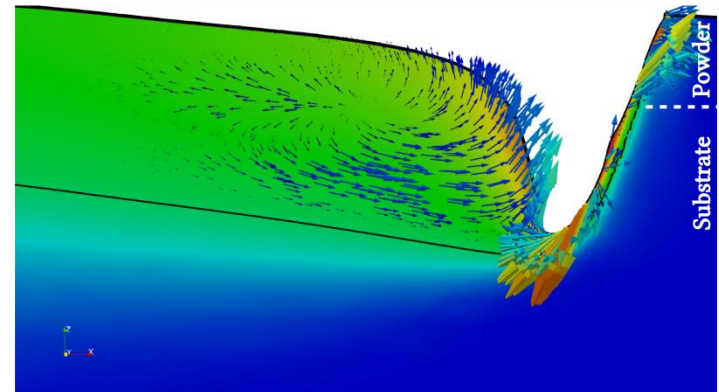
$$N_{Eelts}(t_{end}) = 2.6 \text{ M}$$



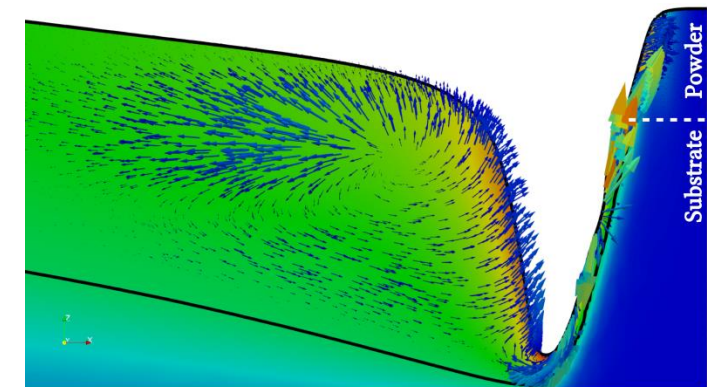
IN738, $\phi_L = 100 \mu\text{m}$



$P_L = 230 \text{ W}, v_L = 960 \text{ mm/s}$
 0.24 J/mm
 $A = 0.70$



$P_L = 320 \text{ W}, v_L = 1100 \text{ mm/s}$
 0.29 J/mm
 $A = 0.79$

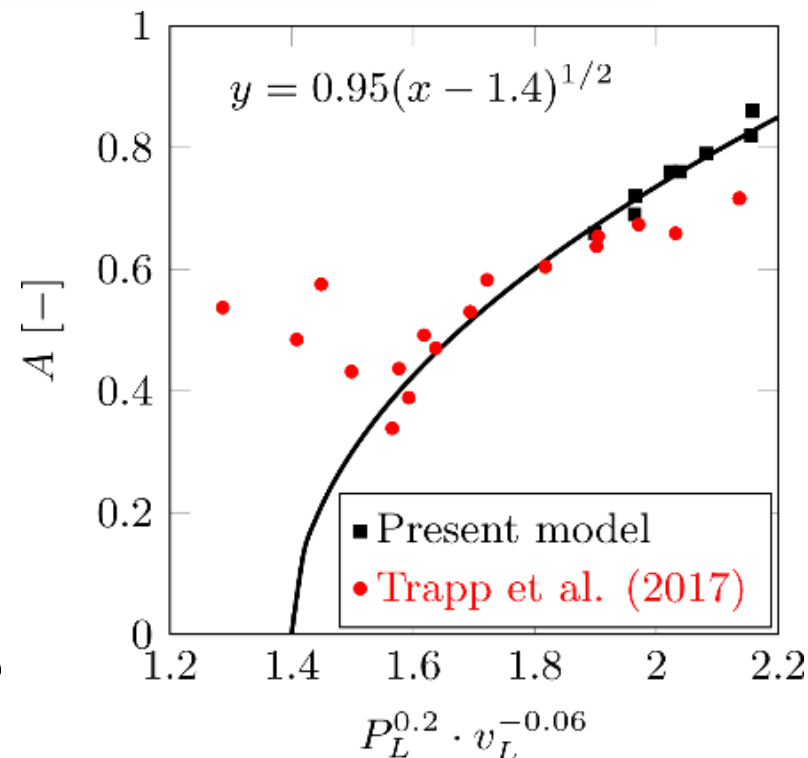
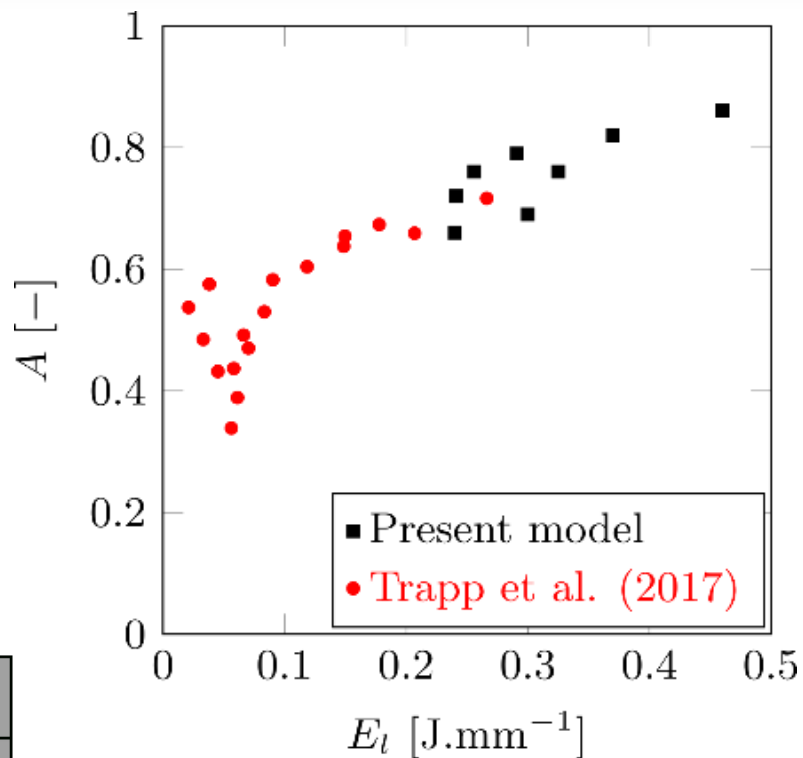
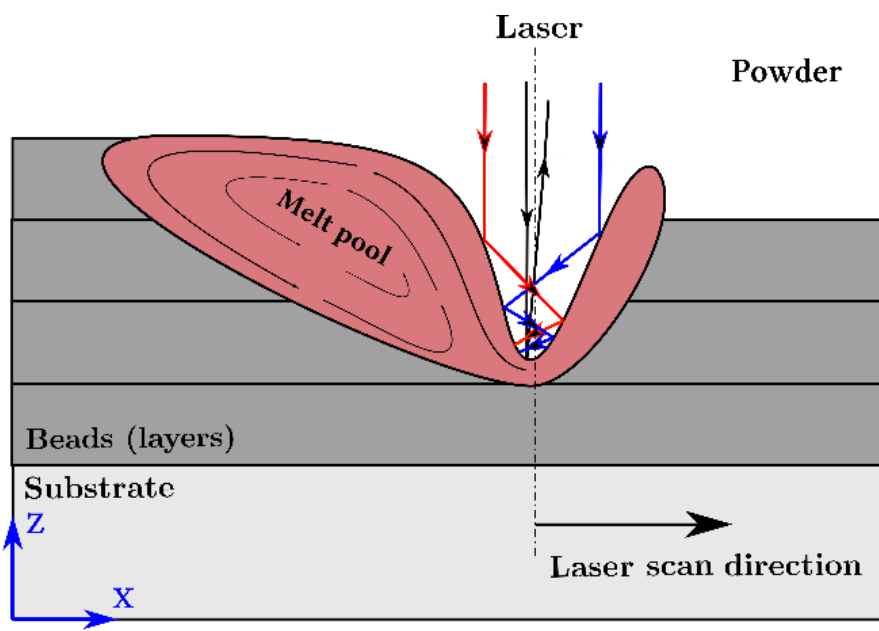


$P_L = 340 \text{ W}, v_L = 730 \text{ mm/s}$
 0.47 J/mm
 $A = 0.82$

Evaluation of the absorption coefficient

- Augmentation of A with keyhole formation

$$E_l = \frac{P_L}{v_L} \nearrow \Rightarrow \text{keyhole} \nearrow \Rightarrow A \nearrow$$



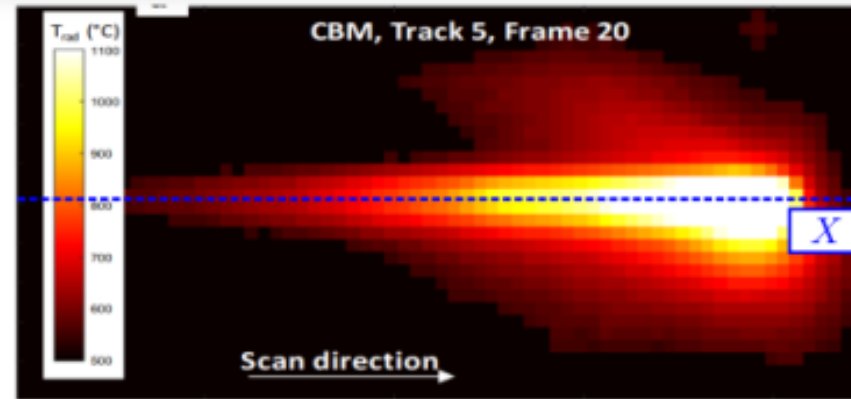
$$A = 0.95 \sqrt{P_L^{0.2} v_L^{-0.06} - 1.4}$$

with P_L [W] and v_L [mm s⁻¹]

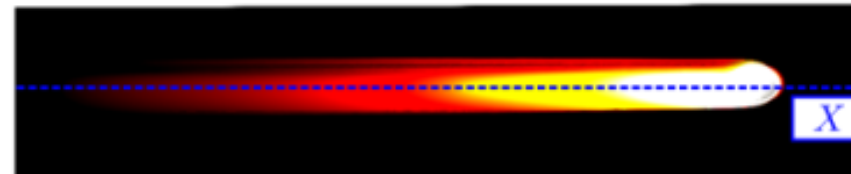
Thermal validation for metals: IR imaging

- Temperature distribution
- Extension of melt pool

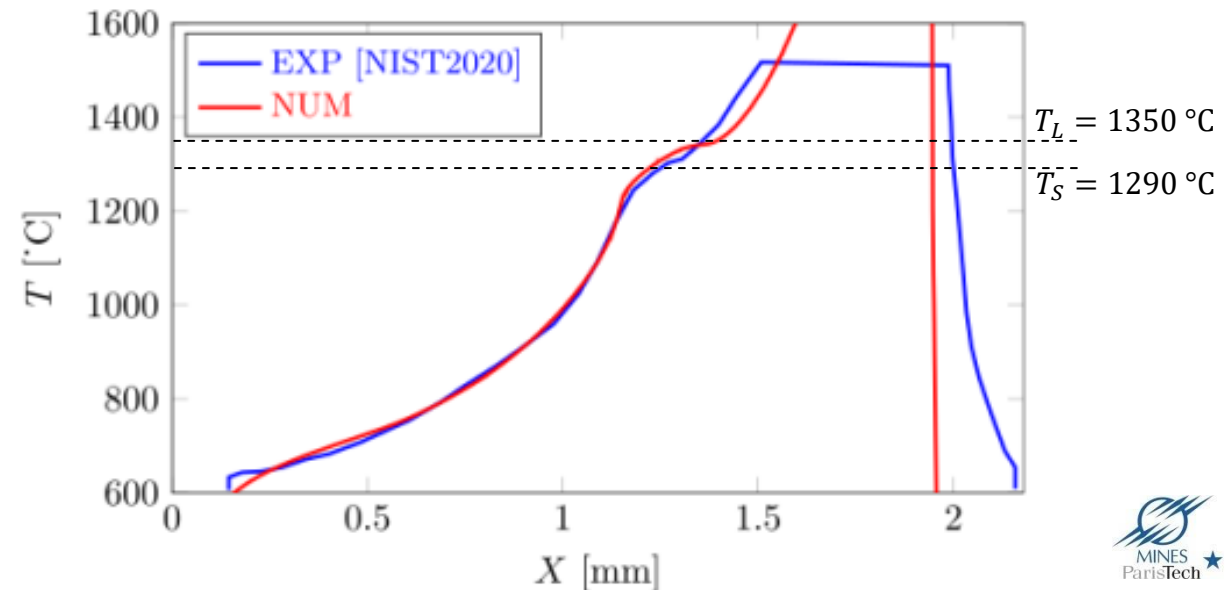
Experimental
NIST: Lane *et al.* 2020



IN625
 $P_L = 195 \text{ W}$
 $v_L = 800 \text{ mm s}^{-1}$
 $\phi_L = 100 \text{ }\mu\text{m}$

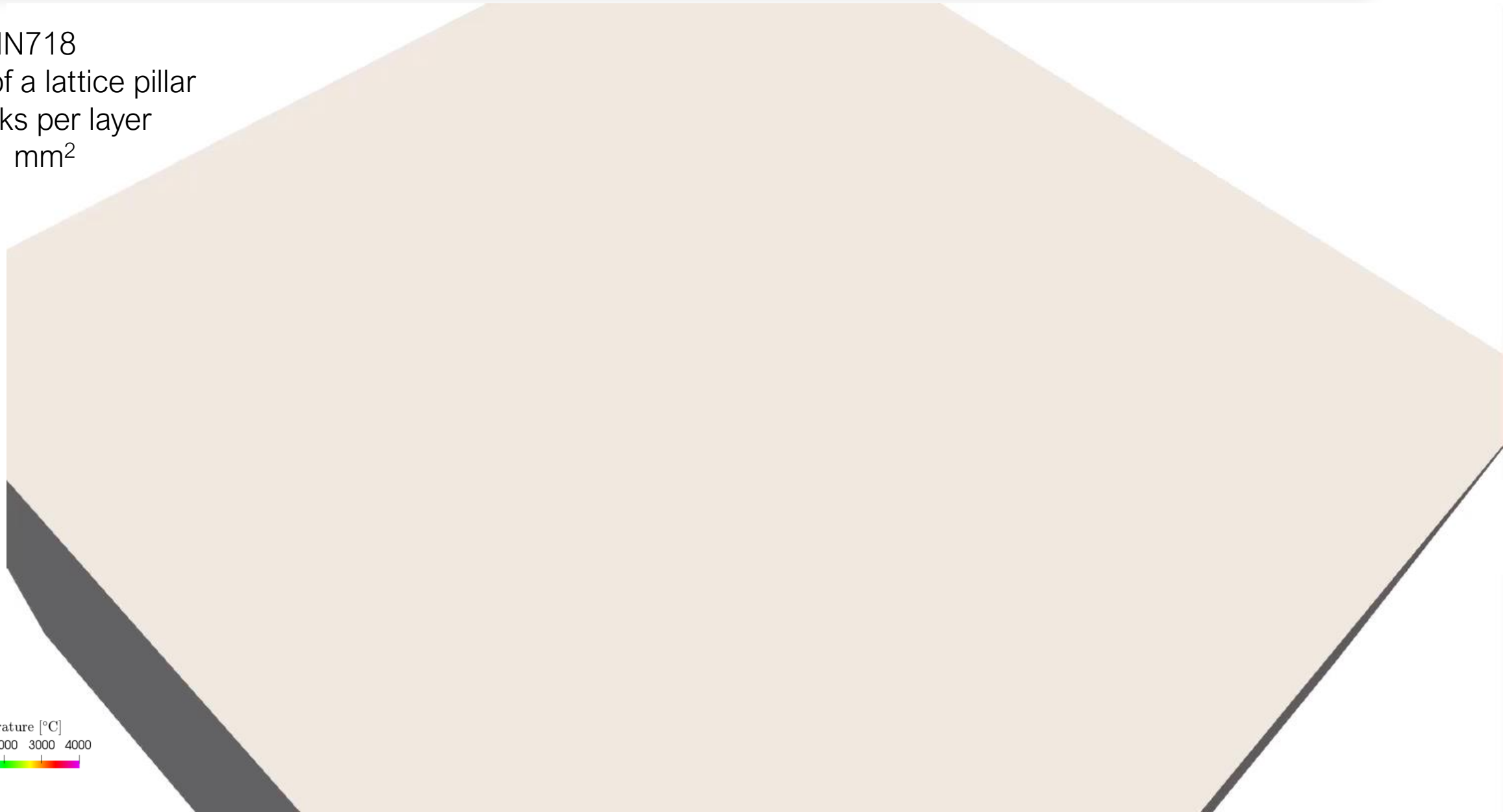
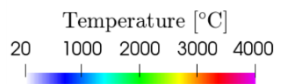


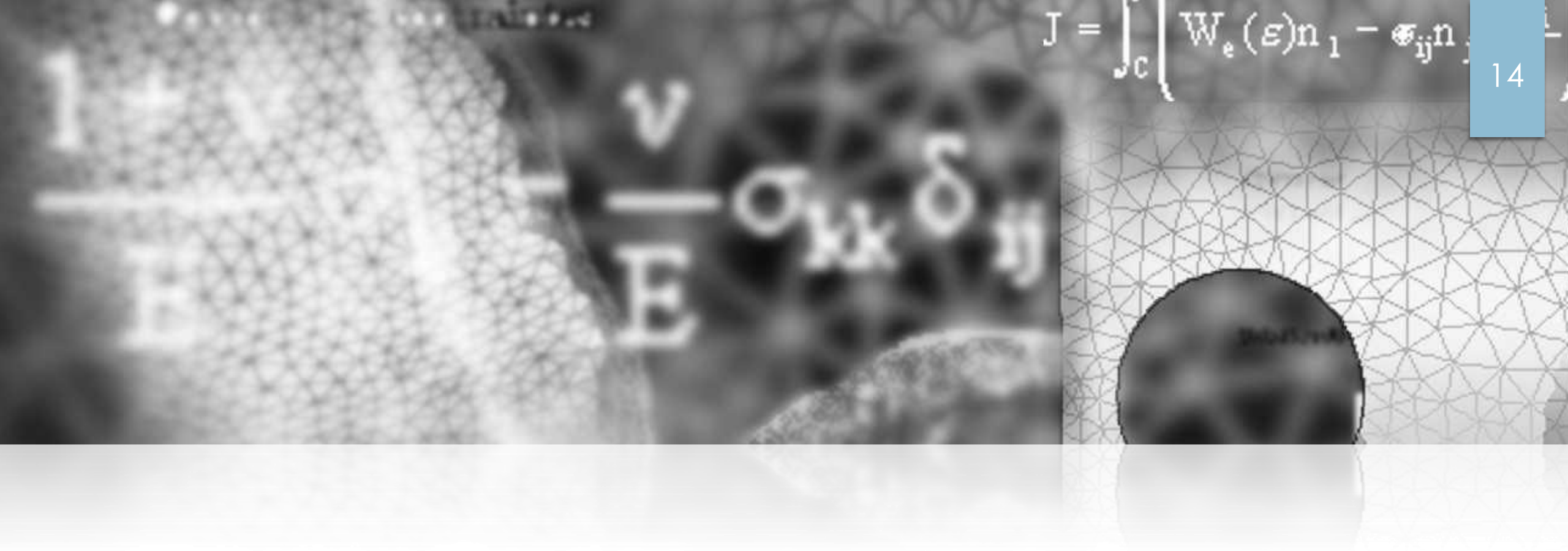
Modelling



Extension to multiple tracks...

IN718
3 layers of a lattice pillar
9 tracks per layer
1 mm²





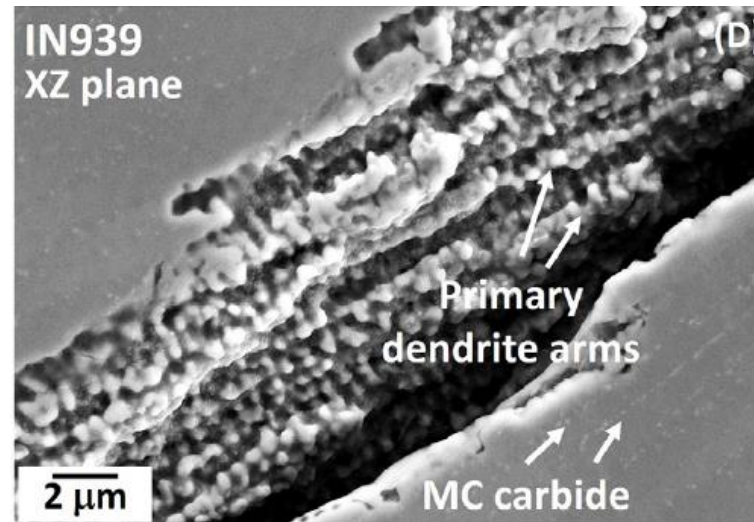
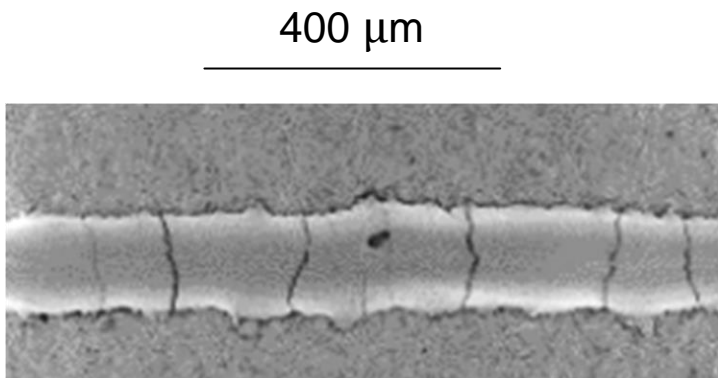
Meso approach: solid mechanics

Why solid mechanics at the meso scale?

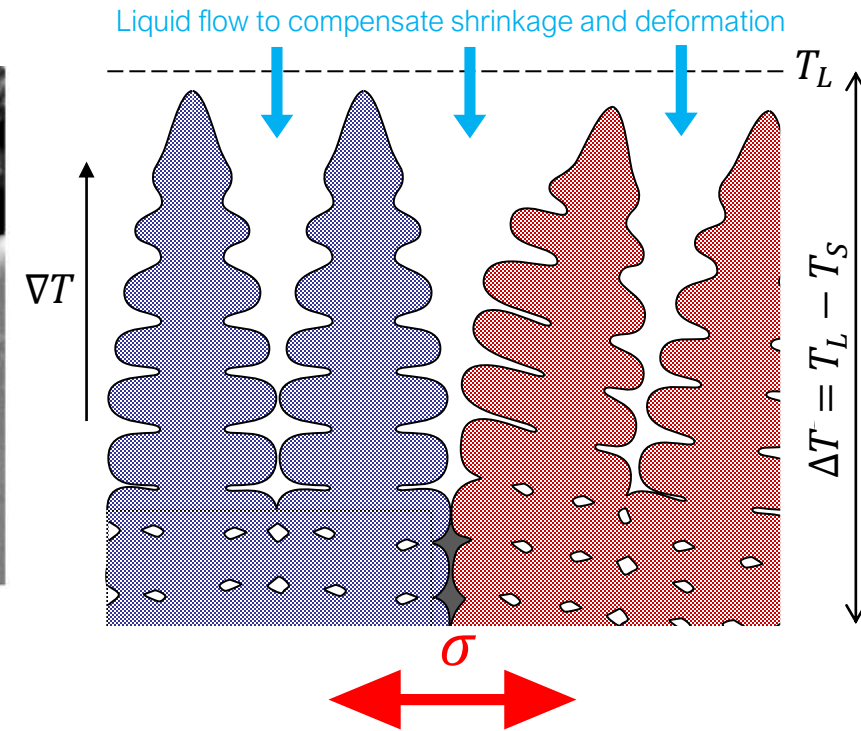
► Required for analysis of

- Cold cracking
- Solidification cracking

result of local stress build-up in the wake or the laser, at the rear of the melt pool



Tang et al., Acta Mater 2021

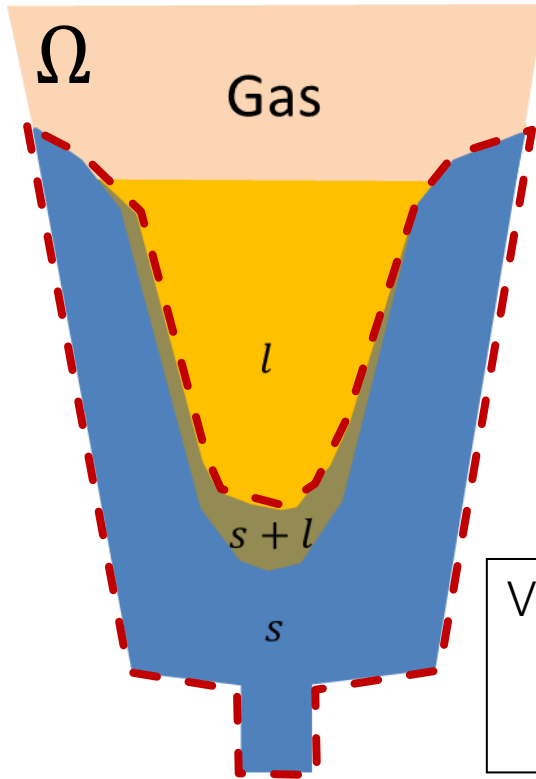


What is needed:

- A solver for solid mechanics
- A constitutive model + material data
- A criterion for cracking

■ PhD Shaojie Zhang (2020)

▶ STEP I: solid mechanics



- ▶ Solid: elastic-viscoplastic
- ▶ Mush: non-Newtonian fluid, homogenized
- ▶ Liquid & Gas: Newtonian fluids, augmented viscosity

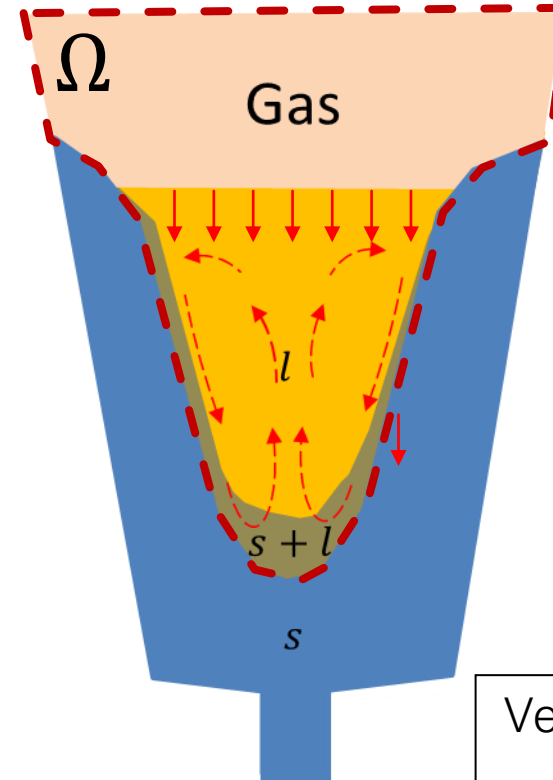
Velocity and pressure calculated on the whole domain Ω :

$$(\mathbf{v}_I, p_I)$$

→ In the solid and the mush:

$$\mathbf{v}_I, \boldsymbol{\sigma}_I, \boldsymbol{\varepsilon}_I$$

▶ STEP II: fluid mechanics



- ▶ Navier-Stokes eqs., spatially averaged (2-phase in the mush)
- ▶ Darcy terms
- ▶ Compressibility (solidification shrinkage)
- ▶ Liquid: nominal viscosity
- ▶ Solid: Newtonian, arbitrary high viscosity

Velocity and pressure calculated on the whole domain Ω :

$$(\mathbf{v}_{II}, p_{II})$$

→ In the mush, the liquid and the gas: \mathbf{v}_{II}, p_{II}

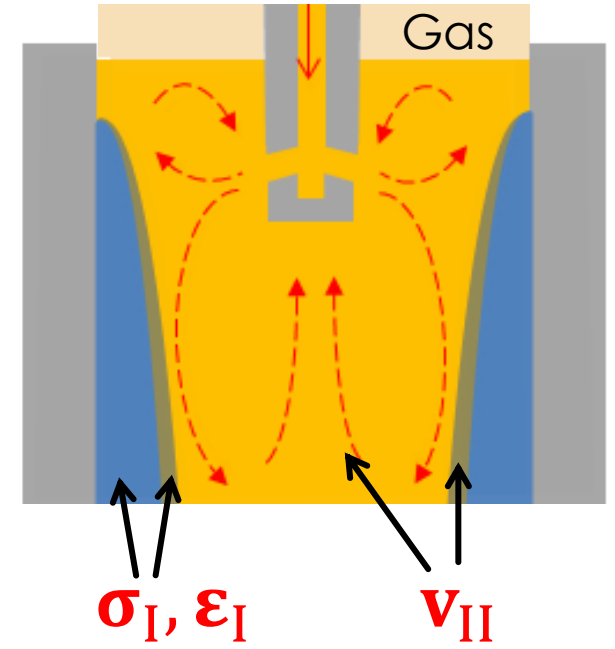
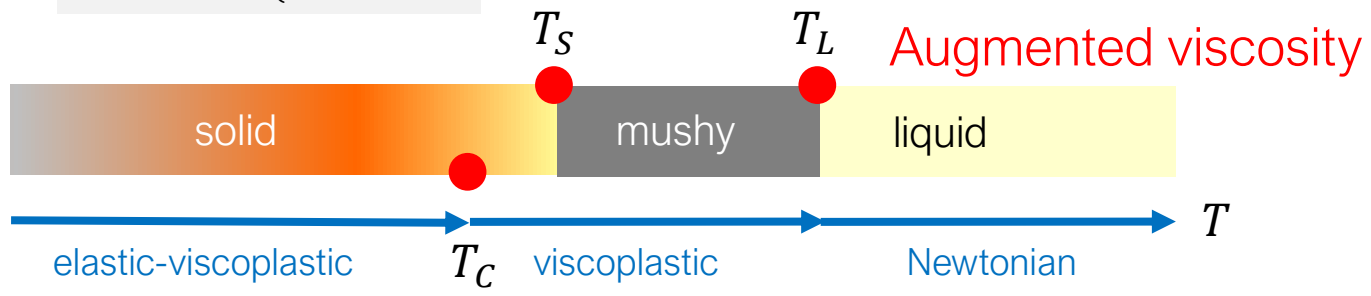
STEP I: solid mechanics

Non-linear

$$\begin{cases} \nabla \cdot \mathbf{s} - \nabla p + \rho \mathbf{g} = 0 \\ \nabla \cdot \mathbf{v} = \text{tr}(\dot{\boldsymbol{\epsilon}}_{th}) + H(T_C - T)\text{tr}(\dot{\boldsymbol{\epsilon}}_{el}) \end{cases}$$

→ (\mathbf{v}_I, p_I)

$$H(T_C - T) = \begin{cases} 0 & T > T_C \\ 1 & T \leq T_C \end{cases}$$



STEP II: fluid mechanics

Nominal viscosity

$$\begin{cases} \langle \rho \rangle^l \left(\frac{\partial \langle \mathbf{v}^l \rangle}{\partial t} + \frac{1}{g^l} (\nabla \langle \mathbf{v}^l \rangle) \langle \mathbf{v}^l \rangle \right) = -g^l \nabla \langle p \rangle^l + \nabla \cdot \langle \mathbf{s}^l \rangle - g^l \mu^l K^{-1} (\langle \mathbf{v}^l \rangle - g^l \langle \mathbf{v} \rangle^s) + g^l \langle \rho \rangle^l \mathbf{g} \\ \nabla \cdot \langle \mathbf{v}^l \rangle = -\frac{1}{\langle \rho \rangle^l} \left(\frac{\partial \langle \rho \rangle^M}{\partial t} + \langle \mathbf{v}^l \rangle \cdot \nabla \langle \rho \rangle^l + \nabla \cdot (g^s \langle \rho \rangle^s \langle \mathbf{v} \rangle^s) \right) \end{cases}$$

Linear!

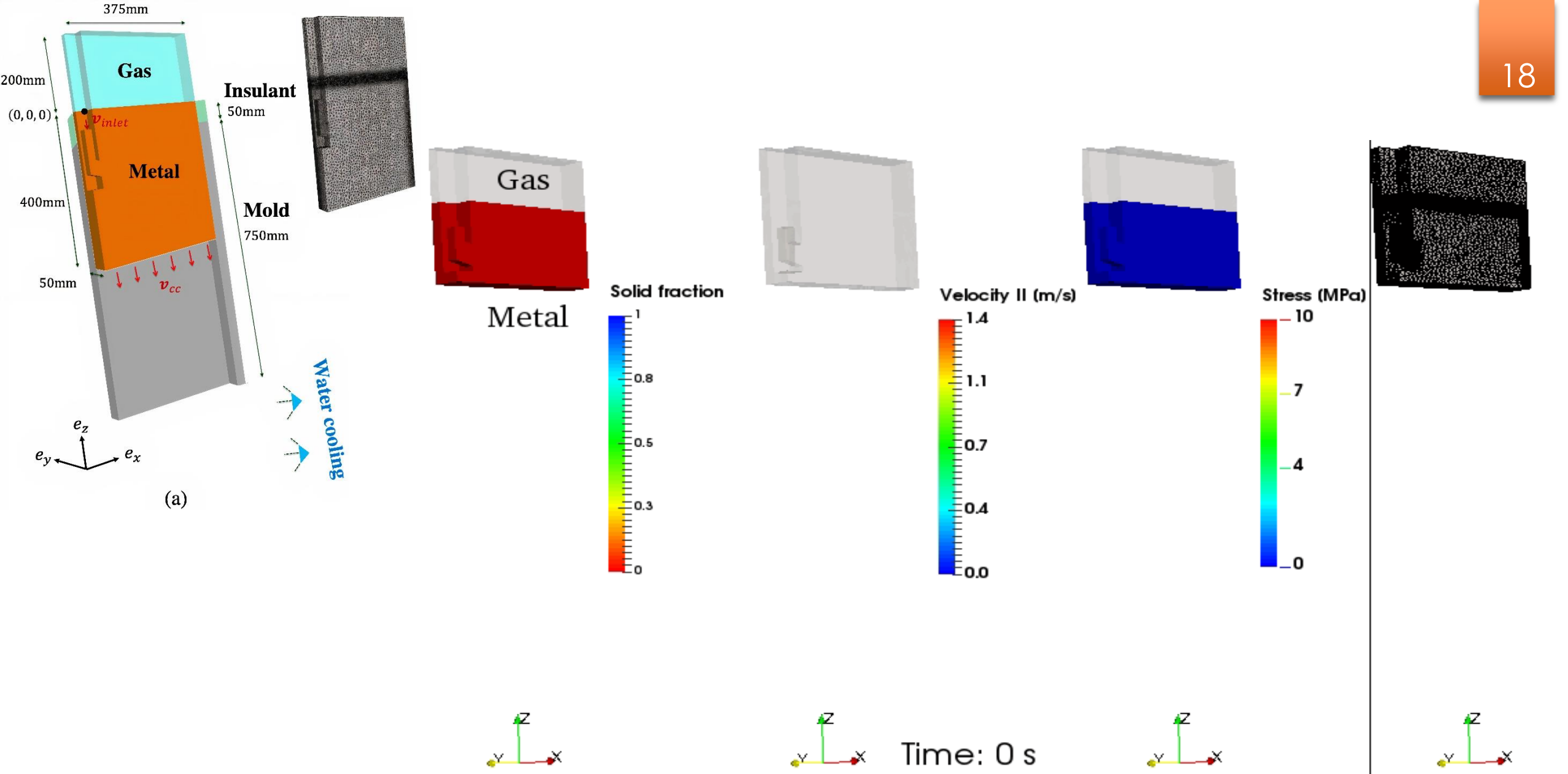
→ $(\mathbf{v}_{II}, p_{II})$

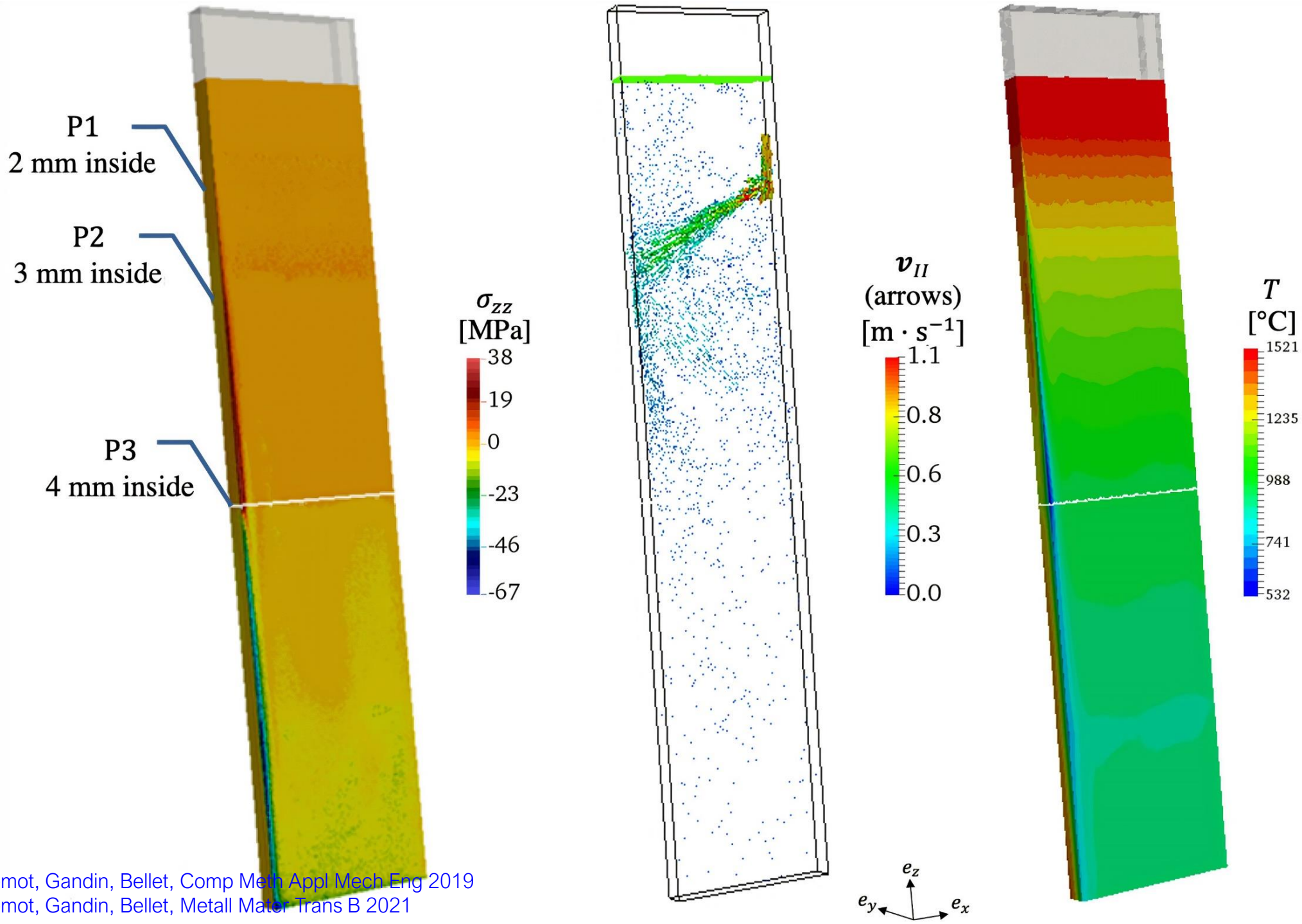
\mathbf{v}_I as an input:

in fully solid regions,
 $\mathbf{v}_{II\text{imp}} = \mathbf{v}_I$

in Darcy term,
 $g^l \langle \mathbf{v} \rangle^s = \mathbf{v}_I$

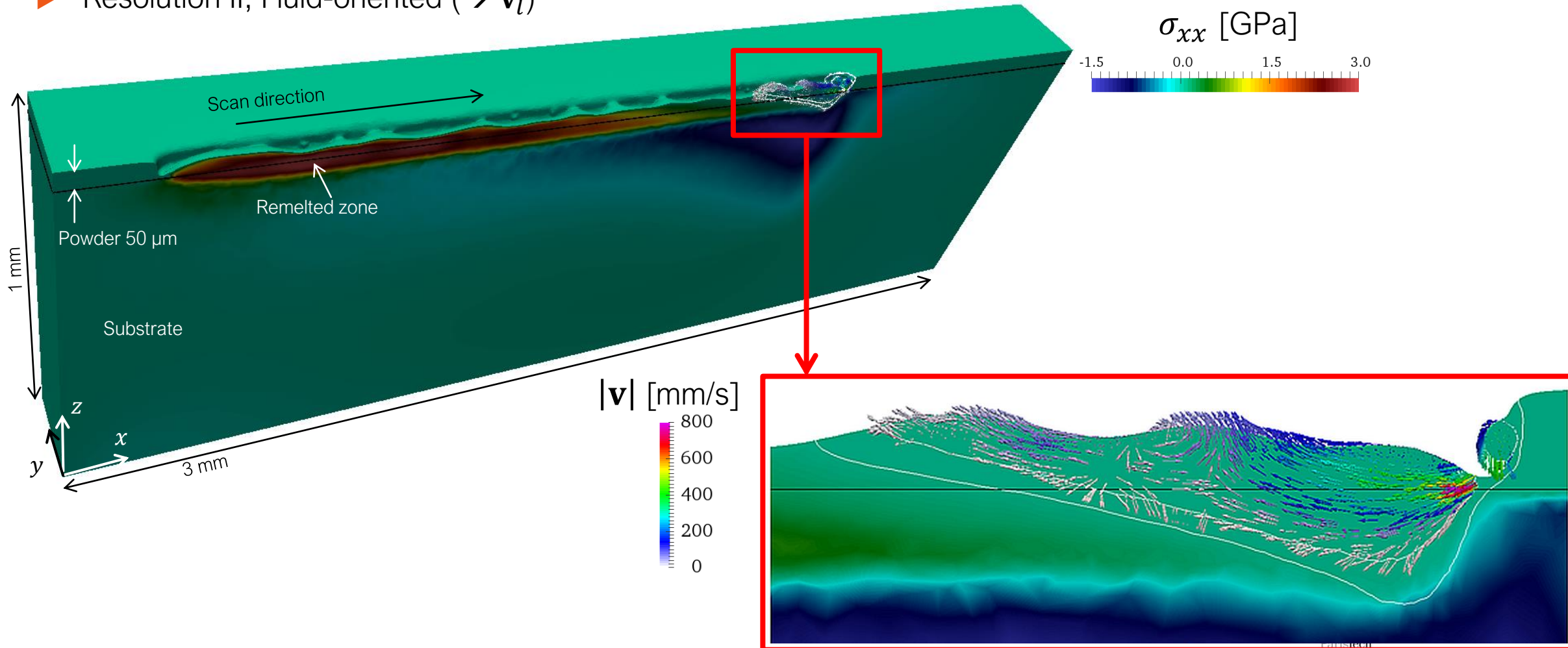
in mass conservation,
 $\langle \mathbf{v} \rangle^s = \mathbf{v}_I$





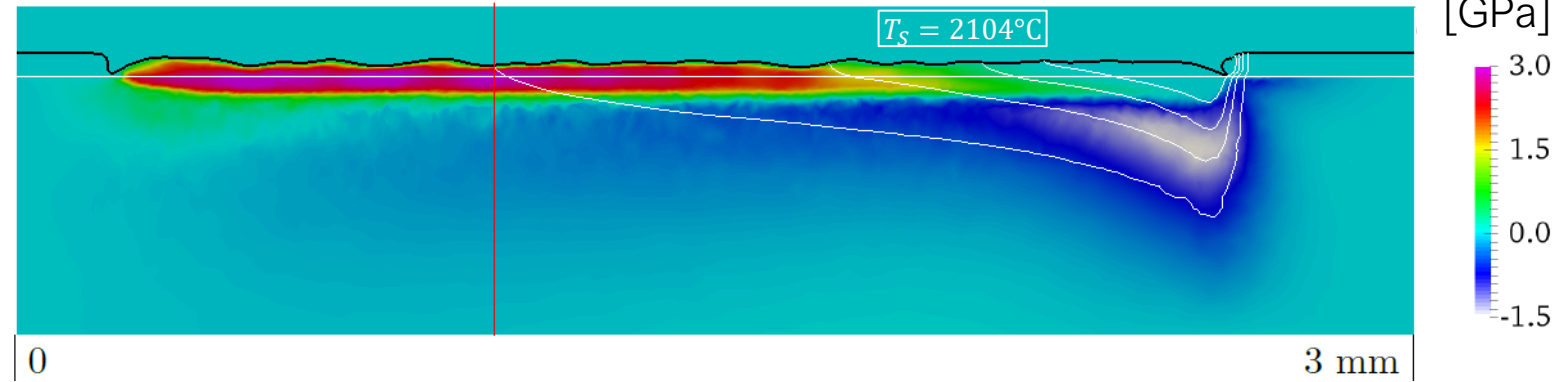
Results : solid thermomechanics + fluid flow in melted zone

- ▶ *Ceramic L-PBF*
- ▶ *Two-step mechanical resolution, at each time step, on the whole domain*
 - ▶ Resolution I, Solid-oriented ($\rightarrow \mathbf{v}_s, \boldsymbol{\sigma}$)
 - ▶ Resolution II, Fluid-oriented ($\rightarrow \mathbf{v}_l$)



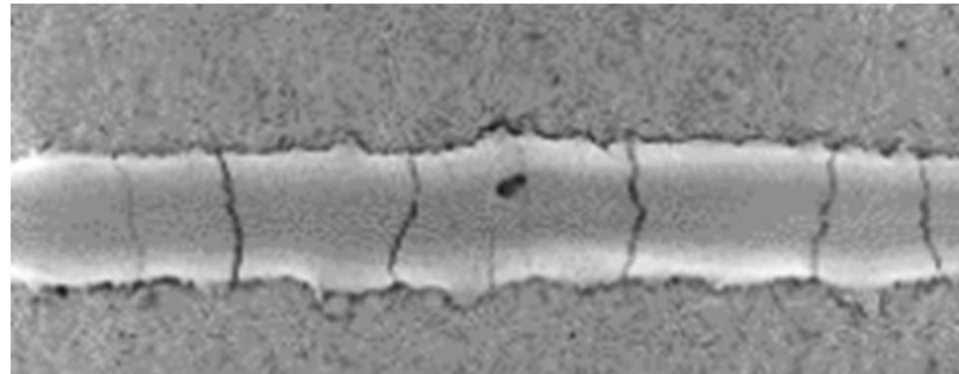
Stress generated, and impact of additional heating

- ▶ Fusion laser $P_L = 84 \text{ W}$, $\phi_L = 100 \text{ }\mu\text{m}$,
 $v_L = 300 \text{ mm s}^{-1}$



Axial stress σ_{xx}

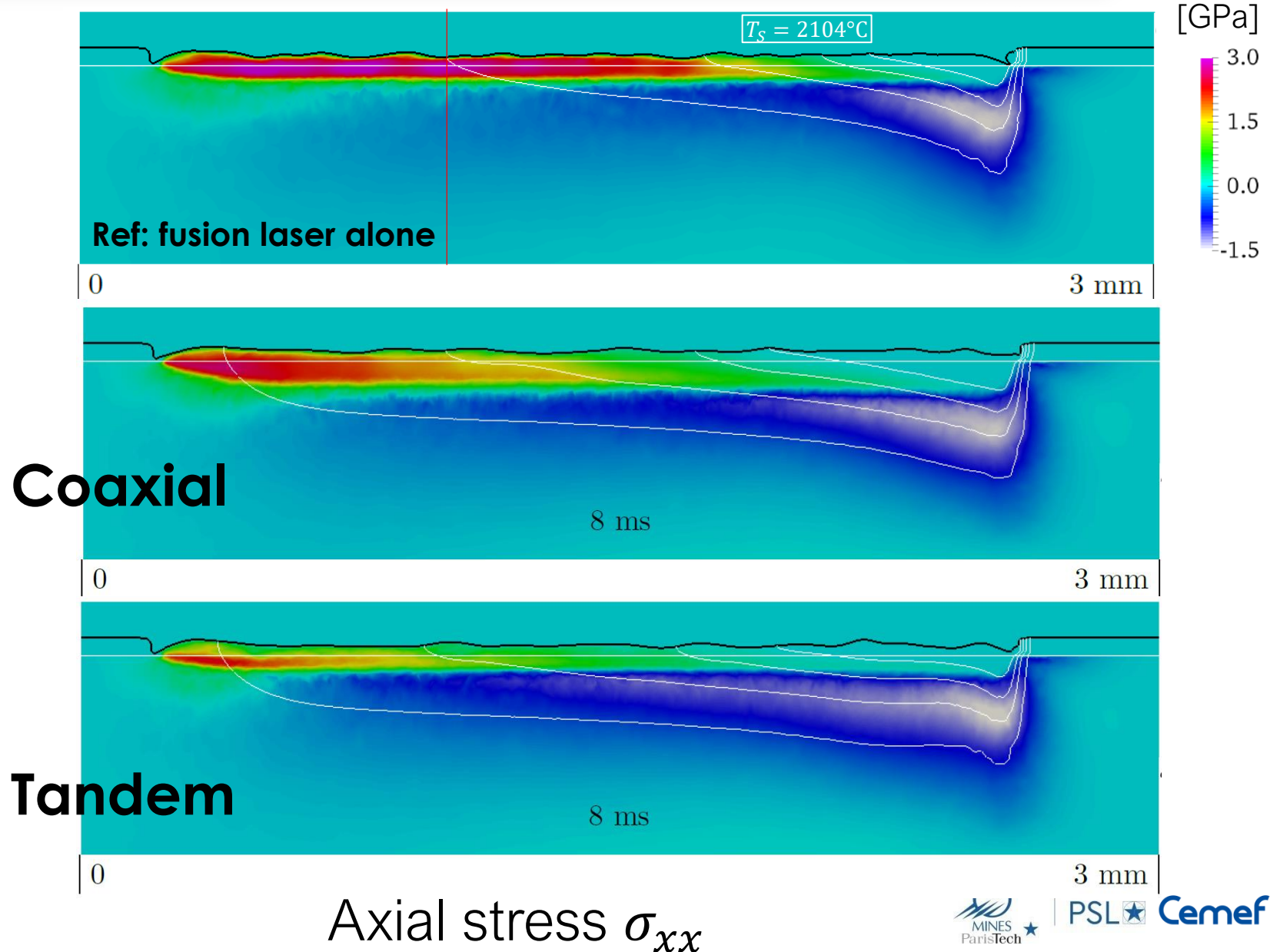
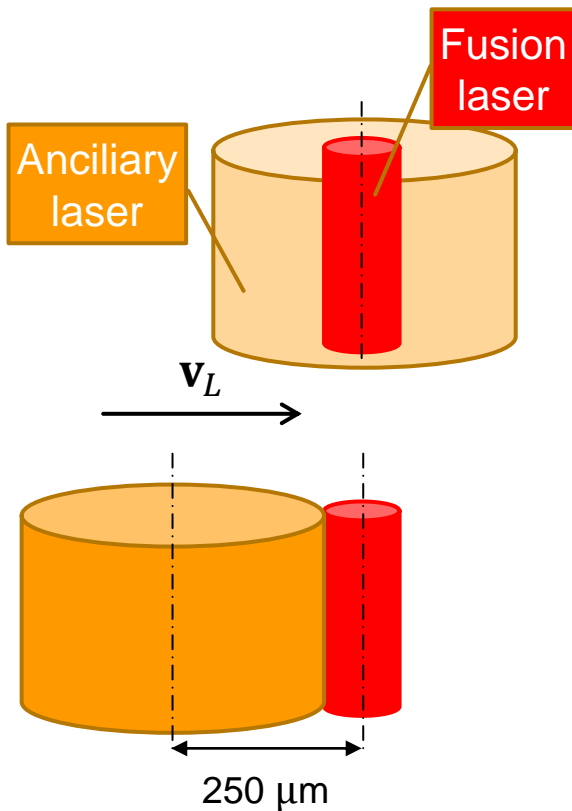
400 μm



Stress generated, and impact of additional heating

▶ Fusion laser $P_L = 84 \text{ W}$, $\phi_L = 100 \text{ }\mu\text{m}$,
 $v_L = 300 \text{ mm s}^{-1}$

▶ 2nd laser $P_L = 60 \text{ W}$, $\phi_L = 400 \text{ }\mu\text{m}$





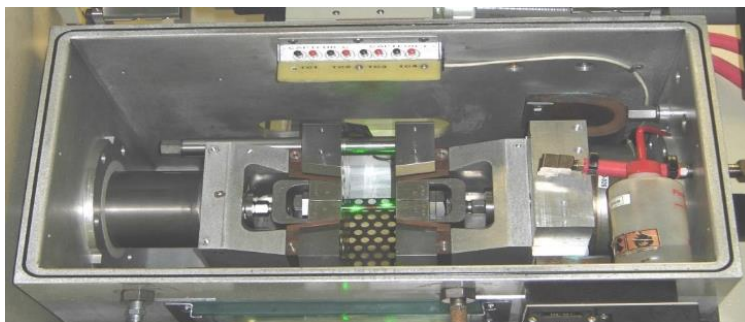
$$J = \int_C \left[W_e(\varepsilon) n_1 - \sigma_{ij} n_j \right]$$

Mechanical characterization, for metals,
at high temperature, for L-PBF simulation

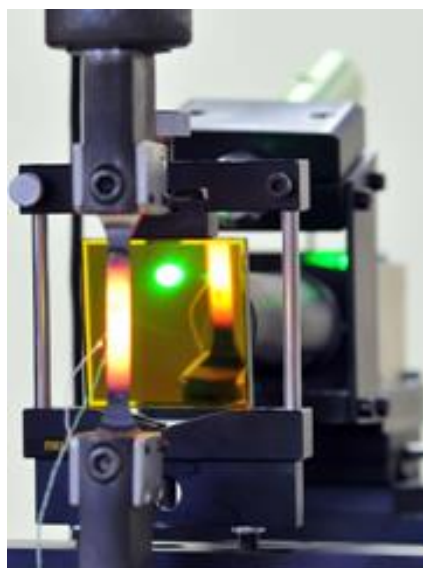
High temperature mechanical characterization

■ Testing under resistive heating

- ✓ Gleeble® machines
- ✓ Specific machines, lab-customized

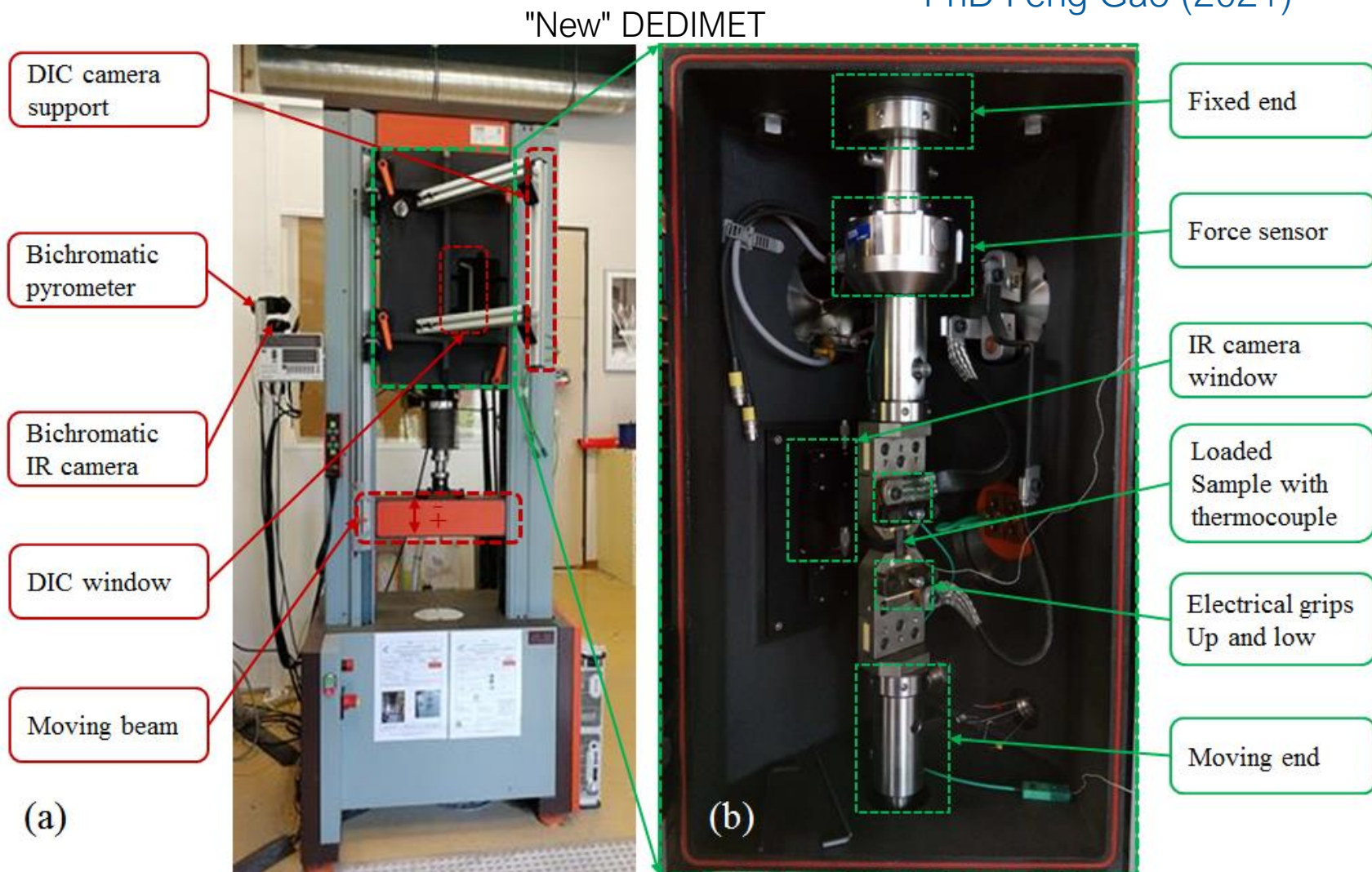


Gleeble® machine

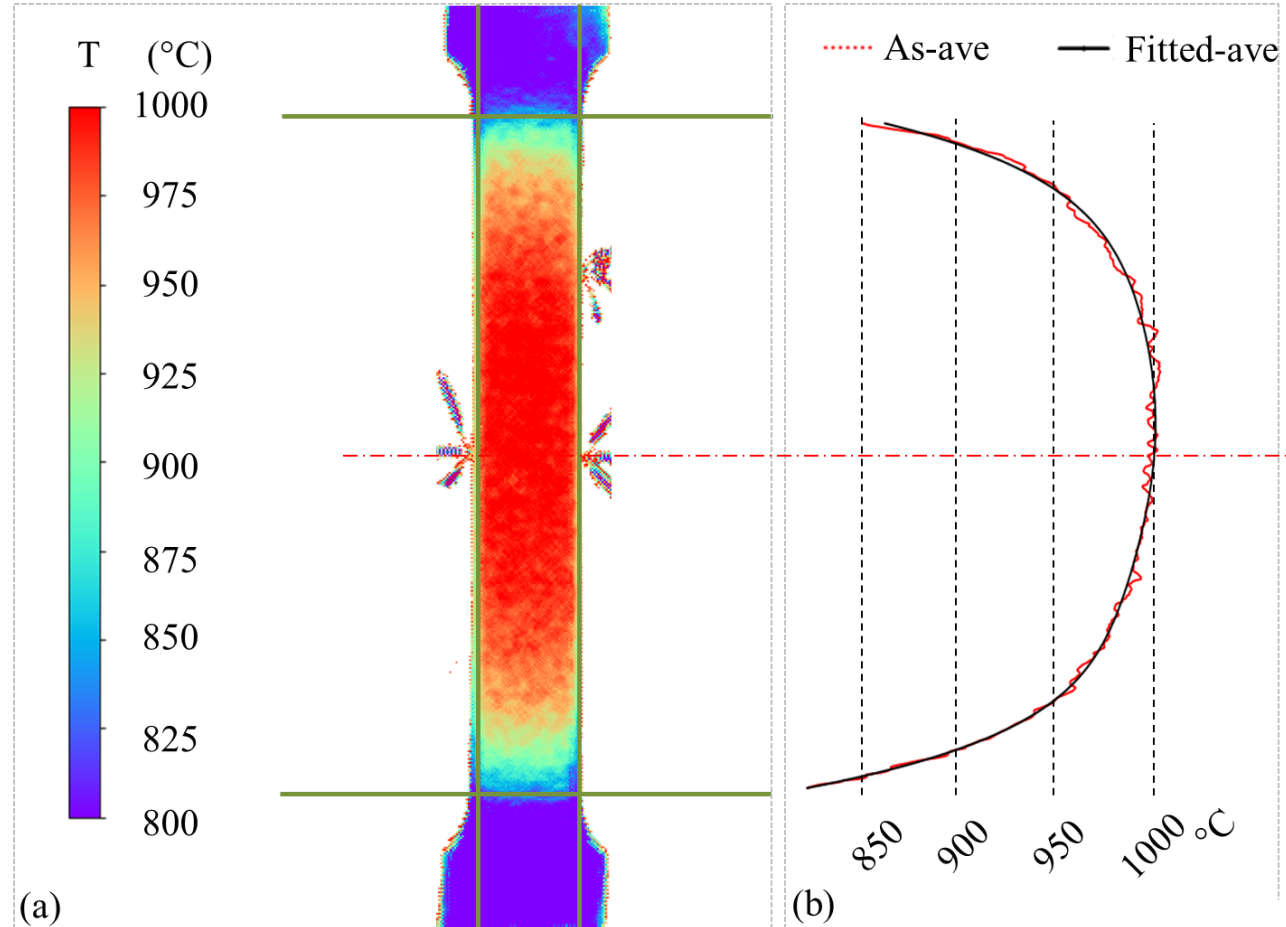


"Old" TABOO (CEMEF)

■ PhD Feng Gao (2021)



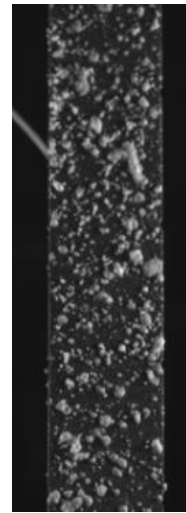
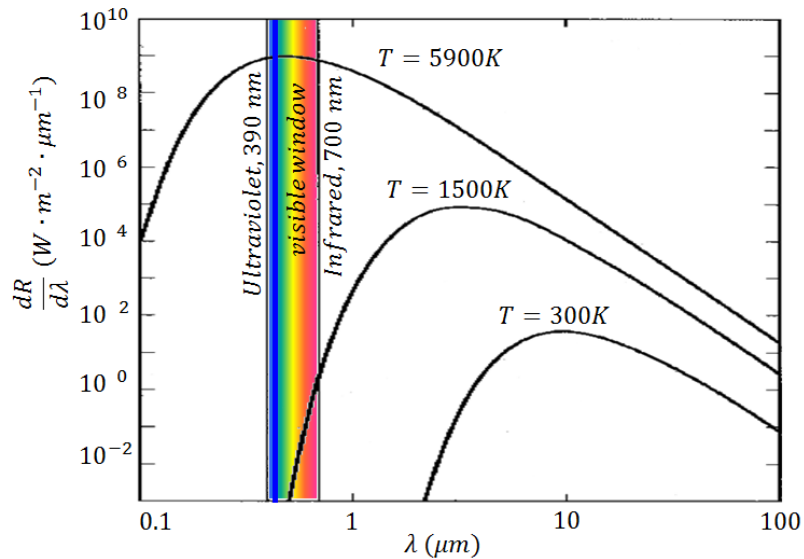
Superalloy IN718,
as-fabricated by
L-PBF



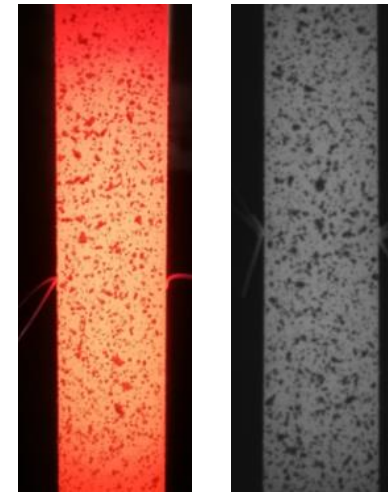
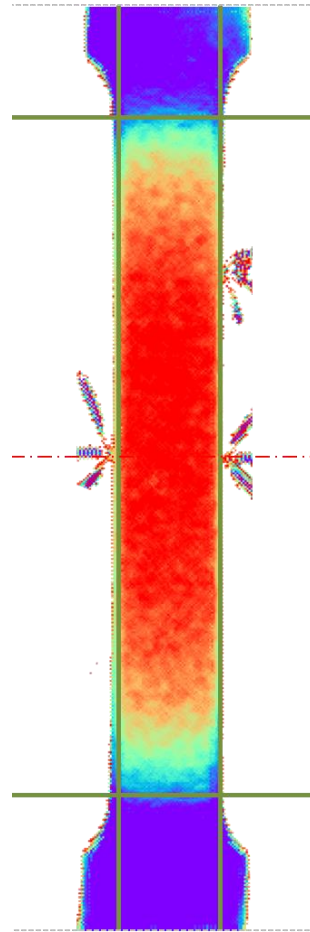
Infra-red imaging

- Testing in presence of $\nabla T \rightarrow$ non-uniform! \rightarrow inverse analysis, by FEM

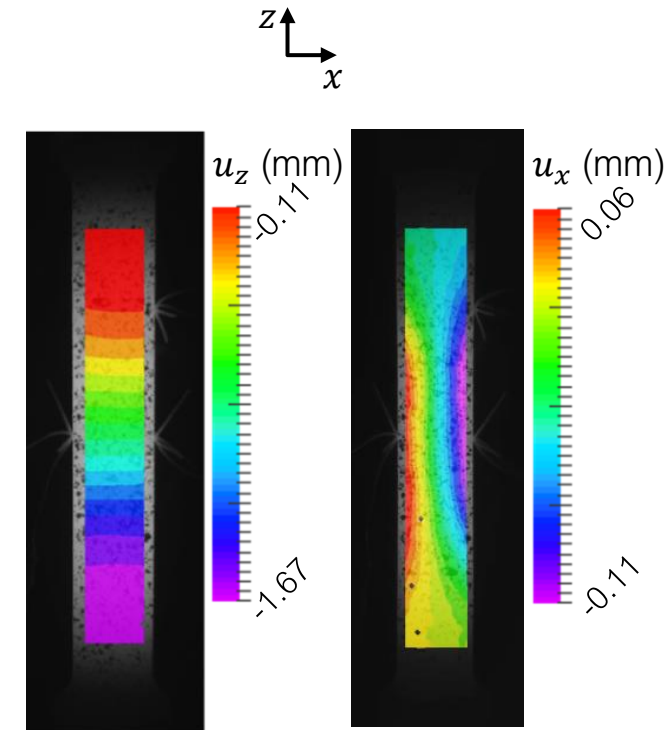
■ Specific DIC technique



Under blue lighting
< 900 °C



Self-emitting
> 800 °C

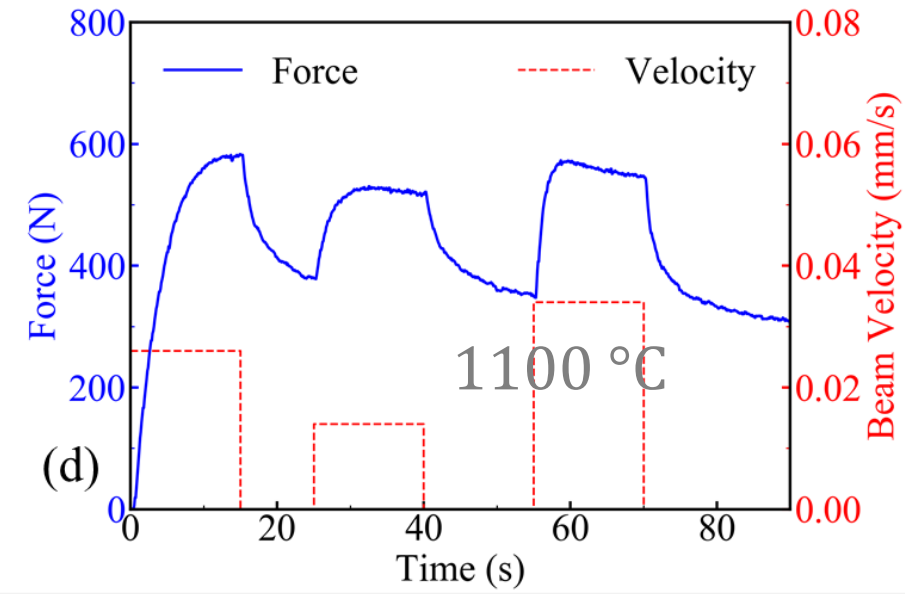
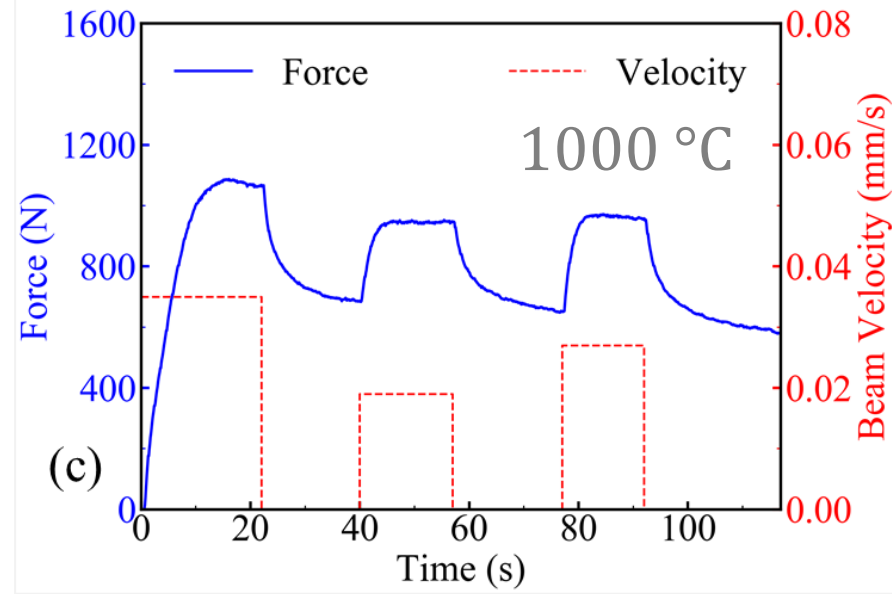
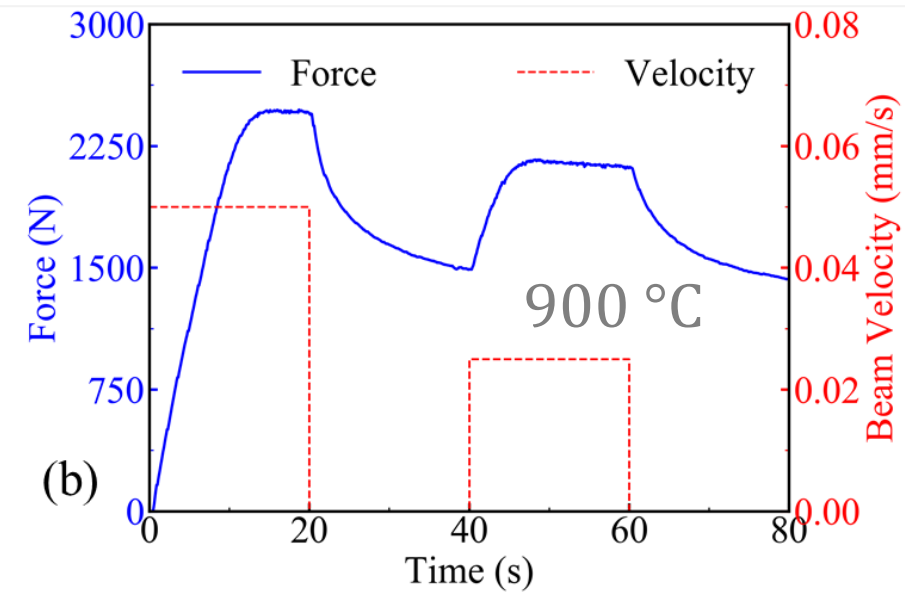
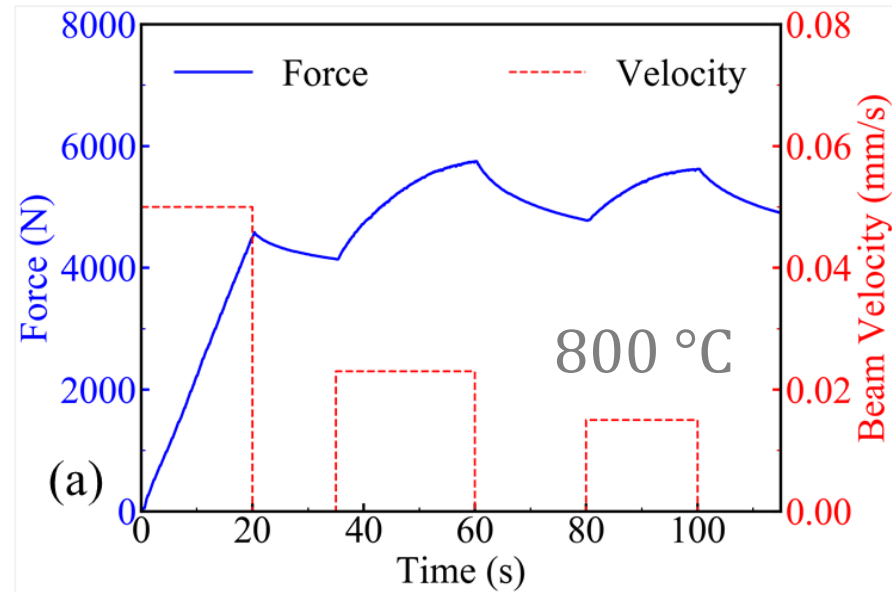


Post-treatment VIC-3D

How to identify an elastic-viscoplastic model?

► Experimental data base

- ✓ Successive tractions and relaxations



► Selection of a candidate model

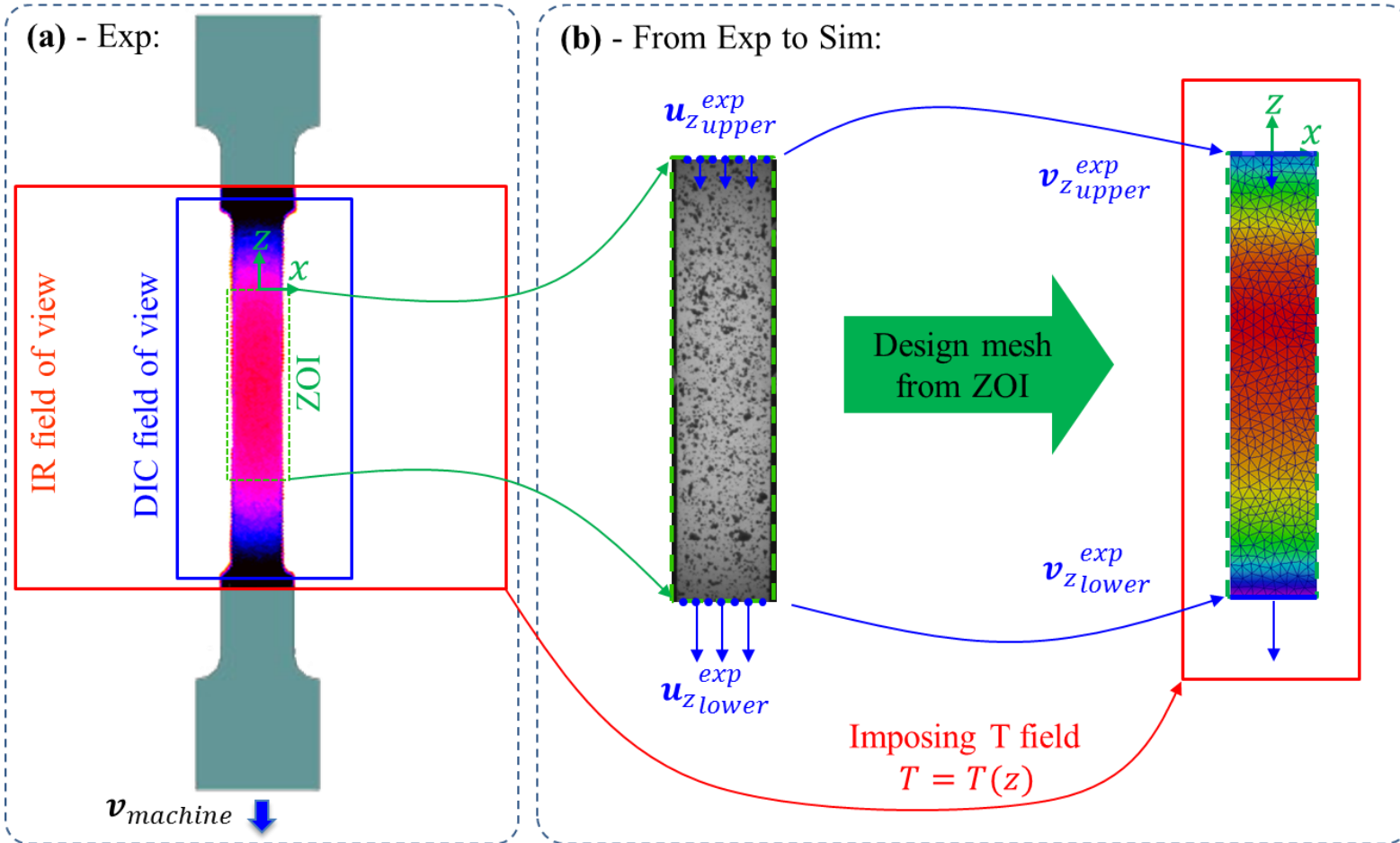
$$\left\{ \begin{array}{l} \dot{\boldsymbol{\varepsilon}} = \dot{\boldsymbol{\varepsilon}}^{th} + \dot{\boldsymbol{\varepsilon}}^{el} + \dot{\boldsymbol{\varepsilon}}^{vp} \\ \dot{\boldsymbol{\varepsilon}}^{th} = \alpha(T) \frac{dT}{dt} \mathbf{I} \\ \dot{\boldsymbol{\varepsilon}}^{el} = \frac{1+\nu}{E} \dot{\boldsymbol{\sigma}} - \frac{\nu}{E} \text{tr}(\dot{\boldsymbol{\sigma}}) \mathbf{I} \\ \dot{\boldsymbol{\varepsilon}}^{vp} = \frac{3}{2\bar{\sigma}} \left(\frac{\bar{\sigma} - \sigma_s(\bar{\varepsilon}, T)}{K(T)} \right)^{\frac{1}{m}} \mathbf{s} \end{array} \right. \quad \begin{array}{l} \sigma_s(\bar{\varepsilon}, T) = \left(\sigma_{Y,ref} + Q_{r,ref} (1 - \exp((-b\bar{\varepsilon})) \right) \exp\left(\frac{Q_1}{R_g T} - \frac{Q_1}{R_g T_{ref}} \right) \\ K(T) = K_{ref} \exp\left(\frac{Q_2}{R_g T} - \frac{Q_2}{R_g T_{ref}} \right) \end{array}$$

$$\bar{\sigma} = \underbrace{\left(\sigma_{Y,ref} + Q_{r,ref} (1 - \exp((-b\bar{\varepsilon})) \right) \exp\left(\frac{Q_1}{R_g T} - \frac{Q_1}{R_g T_{ref}} \right)}_{\sigma_s} + \underbrace{K_{ref} \dot{\boldsymbol{\varepsilon}}^m \exp\left(\frac{Q_2}{R_g T} - \frac{Q_2}{R_g T_{ref}} \right)}_{\sigma_{overstress}}$$

✓ A set of parameters to identify

$$\mathbf{p} = \{ \sigma_{Y,ref}, Q_{r,ref}, b, K_{ref}, m, Q_1, Q_2 \}$$

► **Local** inverse analysis procedure



Cost function to be minimized:

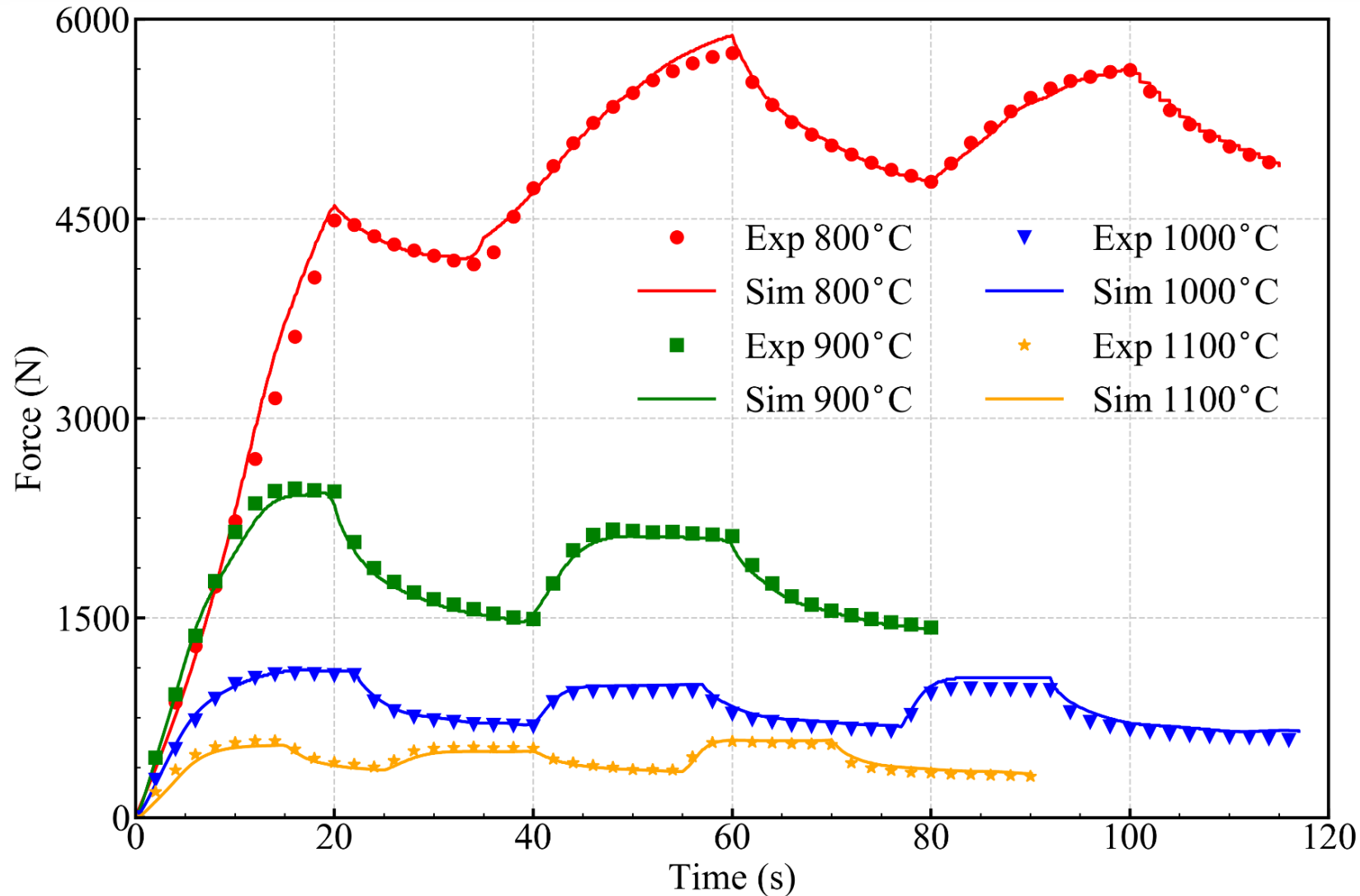
$$\min_{\mathbf{p}} f_c = \sum_{i=1}^N \omega_i \frac{\sum_{j=1}^{M_i} |F_{i,j}^{sim}(\mathbf{p}) - F_{i,j}^{exp}| \Delta t_{i,j}}{\sum_{j=1}^{M_i} F_{i,j}^{exp} \Delta t_{i,j}}$$

Optimisation algorithm: MOOPI (CEMEF)

- Meta-model (response surface)
- Defined by kriging
- Minimization by combining genetic algor. and BFGS

Roux *et al.*, Arch Mech Eng 2020

Results: force vs time at different temperatures



Superalloy IN718,
as-fabricated by
L-PBF

P_{opt}

$$\sigma_{Y,ref} = 107 \text{ MPa}$$

$$Q_{r,ref} = 83 \text{ MPa}$$

$$b = 367$$

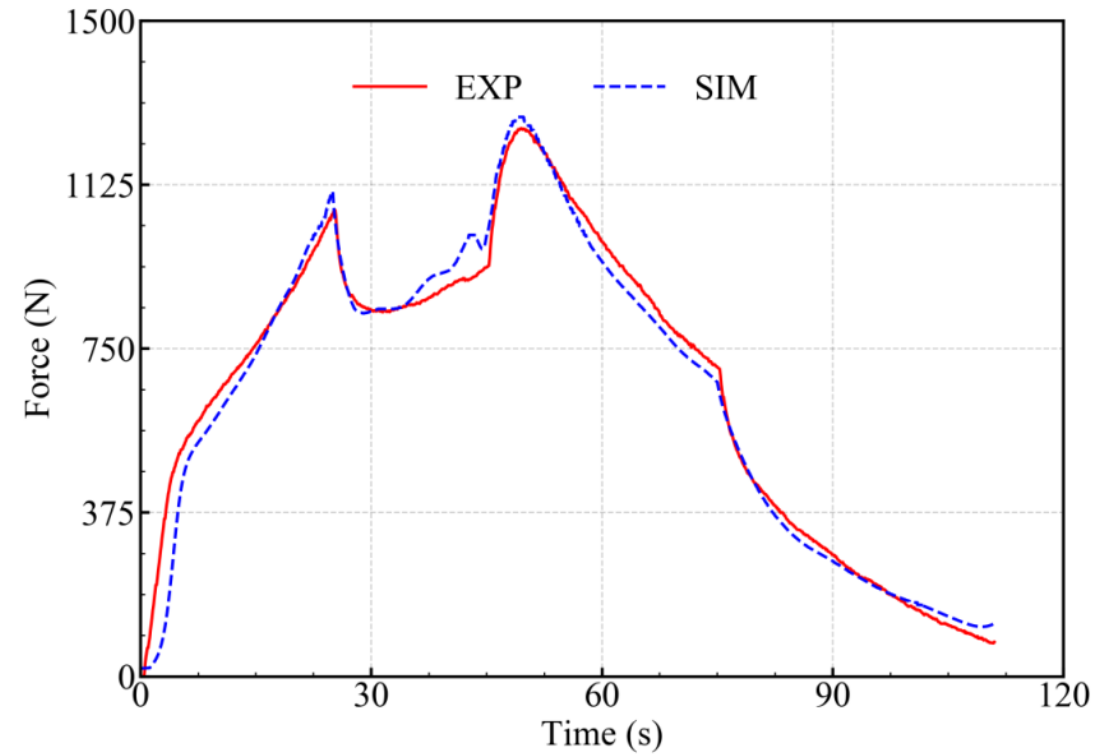
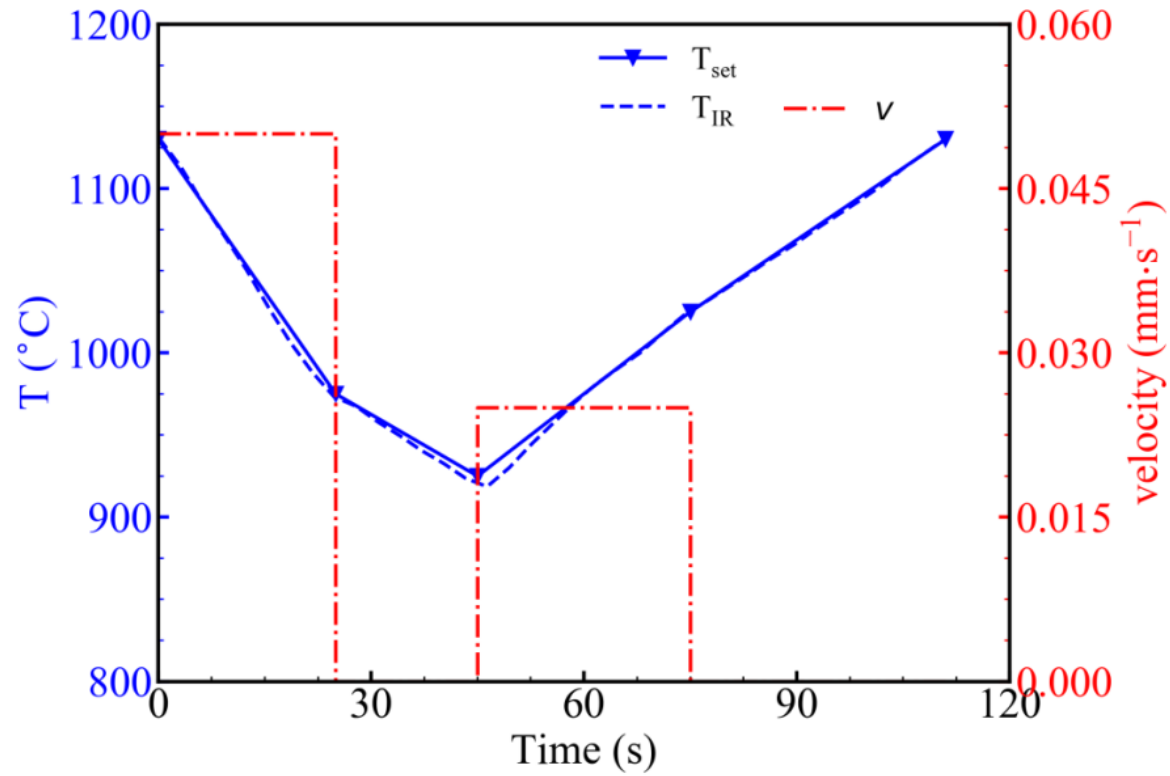
$$Q_1 = 157 \text{ kJ mol}^{-1}$$

$$K_{ref} = 1118 \text{ MPa}$$

$$m = 0.252$$

$$Q_2 = mQ_{vp} = 77 \text{ kJ mol}^{-1}$$

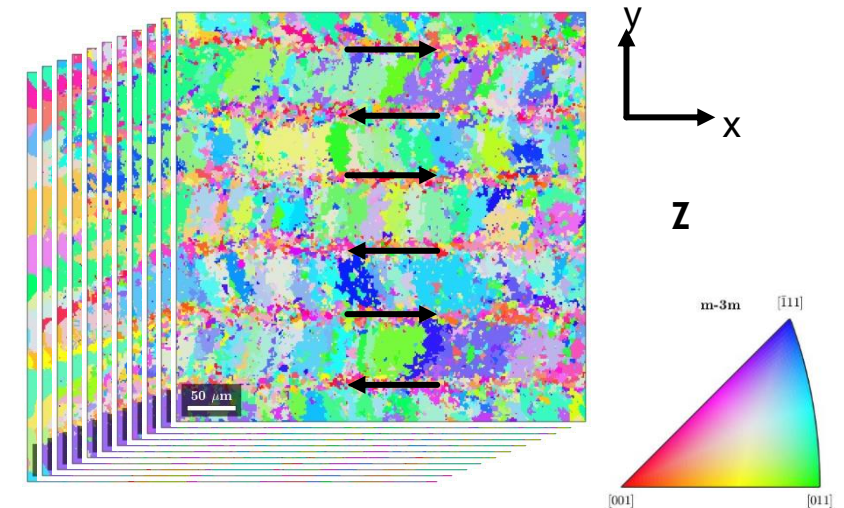
Check for a non-constant temperature case



- ▶ Finite element and level set approach, to model thermohydraulics in L-PBF
- ▶ Concurrent resolution of solid mechanics, in view of determining adequate process windows
- ▶ Local inverse modelling to identify the mechanical behavior of metallic alloys in L-PBF processing conditions

- ▶ Not discussed here ▶ Accounting for anisotropy

- ▶ Next steps
 - ▶ Cracking prediction...
 - ▶ ... enriched by coupling with simulation of microstructure formation
 - ▶ Grain structure prediction by CA-FE modelling
 - ▶ Phases formation in very fast solidification conditions, by CalPhaD (Thermocalc)-based models



Camus, Gandin, Guillemot, 2021 CEMEF

Thank you for your attention !